

**Investigating the Effect of Drilling Parameters and  
Mud Rheology for the Flow of Yield Power Law Fluid  
through Annulus**

by

Nigel Chuah Chung Yang

15940

Dissertation submitted in partial fulfillment of  
the requirements for the  
Bachelor of Engineering (Hons)  
Mechanical Engineering

APRIL 2016

Universiti Teknologi PETRONAS  
Bandar Seri Iskandar  
31750 Tronoh  
Perak Darul Ridzuan

CERTIFICATION OF APPROVAL

**Investigating the Effect of Drilling Parameters and  
Mud Rheology for the Flow of Yield Power Law Fluid  
through Annulus**

by

Nigel Chuah Chung Yang

15940

A project dissertation submitted to the  
Mechanical Engineering Programme  
Universiti Teknologi PETRONAS  
in partial fulfilment of the requirement for the  
BACHELOR OF ENGINEERING (Hons)  
MECHANICAL ENGINEERING

Approved by,

---

(Ir Dr Tamiru Alemu Lemma)

UNIVERSITI TEKNOLOGI PETRONAS  
TRONOH, PERAK

APRIL 2016

**Certificate of Originality**

This is to certify that I am responsible for the work submitted in this project, that the original work is my own except as specified in the references and acknowledgement, and that the original work contained herein have not been undertaken or done by unspecified sources of persons.

---

NIGEL CHUAH CHUNG YANG

## **ACKNOWLEDGEMENT**

I would like to express my sincere gratitude to my supervisor, Dr Tamiru Alemu Lemma for his endless guidance and support throughout the Final Year Project (FYP) course which ran for two consecutive semesters. Under his guidance, I am able to complete my FYP within the time frame given which is seven months and conduct the experiment in a conducive manner.

I would like to thank UTP for providing this course to final year students as it teaches students on how to apply their theoretical engineering knowledge into practice. As a final year student, it is imperative to apply all the knowledge that has been collected throughout five years of engineering study in UTP. Throughout this FYP course, I have equipped myself with both technical and soft skills through experimental works as well as presentations in which it is very much sought after in the industry.

I also would like to take this opportunity to acknowledge and thank everyone who has been supporting me and giving guidance throughout the period of completion for this project. On top of that, I would like to thank Dr Turnad Linggo Ginta and Dr Tamiru Alemu Lemma, coordinators for Final Year Project 1 and Final Year Project 2 respectively for their efforts in ensuring any arrangements made related to the course is within the scheduled time. Finally, my sincerest gratitude to my fellow colleague for their help and support throughout the course of this project.

## ABSTRACT

Fluid flow in the annulus has been the center of numerous studies, whether from the oil industry or academia. This study deals with numerical simulations using computational fluid dynamics technique to investigate the parameters that affect the pressure gradient in the annulus for the flow of Yield Power Law fluids. The study analyses the effect of cutting concentration through volume fraction, flow rate, inclination, eccentricity and rheological properties of drilling fluid on the pressure losses through the annulus. Previous work in the field of study has provided models which aided the industry to better predict hole cleaning efficiency and pressure losses. The benefits of better pressure loss predictions are well documented with potential millions in saving from drilling optimization with the use of modeling. Some of the more advanced studies have included the kinetic theory of granular flow for example to great effect to model hydrodynamics. With the advent of computational fluid dynamics, highly accurate simulations were conducted to test these models and the results are encouraging, with only minor deviations obtained compared to prior experimental work. Moving forward, the effect of mud properties, velocity, inclination, eccentricity, and cuttings were investigated and discussed. A new correlation was proposed with the use of 2<sup>nd</sup> Order Polynomials, Kriging and Artificial Neural Network (ANN) response surface analysis. Kriging was found to be the best performing response surface, with mud rheology and cutting-volume fraction being the significant source of pressure drop in annulus. Drill pipe rotation was found to play a small part in reducing pressure losses. The effects of inclination and eccentricity were not so clear, with conflicting results obtained from the response surface types used.

## TABLE OF CONTENT

ACKNOWLEDGEMENT .....	4
ABSTRACT.....	5
Table of content .....	6
LIST OF FIGURES .....	9
LIST OF TABLES .....	12
Chapter 1 : INTRODUCTION.....	13
1.1    Background of Study .....	13
1.2    Problem Statement.....	15
1.3    Objectives .....	16
1.4    Scope of study .....	16
Chapter 2 : Literature Review .....	17
2.1    Introduction .....	17
2.2    Drilling Fluids .....	20
2.2.1 Drilling Fluid Functions .....	20
2.2.2 Drilling Fluid Properties.....	21
2.2.3 Power Law Model .....	23
2.2.4 Bingham plastic model.....	24
2.2.5 Hershel Buckley model .....	24
2.2.7 Foam with Quality.....	25
2.3    Computational Fluid Dynamics (CFD) .....	26
2.3.1    CFD Applied to Cutting Transport Predictions.....	27
2.4    Pressure Loss Predictions .....	29
2.5    Borehole Temperature and Pressure.....	29
2.6    Summary.....	32
Chapter 3 : METHODOLOGY .....	33

3.1	Introduction .....	33
3.1.1	Literature Review .....	33
3.1.3	CFD modeling and simulation .....	34
3.1.4	Documentation .....	34
3.2	Transient and Laminar Hydraulic Model for Managed Pressure Drilling .....	34
3.2.1	Fundamental equation and theory .....	35
3.2.1	Benchmark Problem by Ekembara.....	38
3.2.2	Benchmark Problem by Founargiotakis .....	39
3.3	Solution Method and Performance Evaluation Parameters .....	40
3.3.1	Simulating Benchmark Problem by Ekembara .....	40
3.3.2	Simulating Benchmark Problem by Founargiotakis .....	44
3.4	Parametric Study and Regression Analysis .....	47
3.4.1	Design of Experiment and Response Surface .....	48
3.5	Summary.....	50
Chapter 4 : RESULTS AND DISCUSSION .....		52
4.1	Introduction .....	52
4.1.1	Model and Simulation Setting.....	52
4.2	Simulation.....	52
4.2.1	Case-1: Model Verification and Effect of Cutting as a Density and Viscosity Modifier on the Pressure Gradient in Annulus .....	53
4.2.2	Case-2: Effect of cutting volume-fraction, mud flow rate, inclination, drill pipe rotation, and mud rheology on the pressure drop in annulus.....	54
4.2.3	Relationship between Reynolds, Froude, Taylor and Bingham dimensionless numbers and the pressure drop for flow in annulus .....	59

4.3	Discussion.....	64
4.3.1	Influence of mud rheology on pressure drop .....	64
4.3.2	Effect of cutting volume-fraction on pressure drop .....	65
4.3.3	Influence of drilling parameters on pressure drop .....	66
Chapter 5 : CONCLUSION AND RECOMMENDATION .....		68
5.1	Conclusion.....	68
5.2	Recommendation.....	69
REFERENCES .....		70
APPENDIX-A.....		72



## LIST OF FIGURES

Figure 1:1. Time-depth curves for well K-04 in Northern Oman showing improvements compared to the previous offset well.....	14
Figure 2:1 Illustration of cutting bed formation at a horizontal inclination of 90° by Sifferman. ....	18
Figure 2:2. Graph depicting the prominent effect of drill pipe rotation on cutting removal by Sanchez. ....	19
Figure 2:3. Characteristics of different non-Newtonian fluids .....	22
Figure 2:4. Typical non-Newtonian fluid viscosity versus shear rate behaviour.....	22
Figure 2:5. General Fluid Rheological Model .....	23
Figure 2:6. Contour plots for particle concentration taken at regularly spaced axial positions over the 10m control volume. The following conditions were simulated: cutting diameter 90 µm, and liquid velocity 3.0 m/s. ....	28
Figure 2:7. Cutting concentration vs. downhole pressure for 0.8-quality foam with pipe rotation.....	30
Figure 2:8. Pressure drop vs. downhole pressure for 0.8-quality foam with pipe rotation .....	30
Figure 2:9. Cutting concentration vs. downhole temperature for 0.8-quality foam with pipe rotation .....	31
Figure 2:10. Pressure drop vs. downhole temperature for 0.8-quality foam with pipe rotation .....	31
Figure 3:1. Sequential task blocks .....	33
Figure 3:2. Grid structure for the benchmark validation simulation.....	40

Figure 3:3. Predicted liquid velocities for the selected data set by Ekambara.....	42
Figure 3:4. Velocity contour plot from the validation test simulation.....	42
Figure 3:5. Liquid velocity profiles obtained from this project simulation. ....	43
Figure 3:6. Comparison of the liquid velocity profiles obtained by Ekambara (2009) with the validation test result showing resonable agreement. ....	43
Figure 3:7. Simulated Well geometry .....	44
Figure 3:8. Screenshot of the CFX Expressions used to obtain the change in pressure over length.....	45
Figure 3:9. Comparison of predictions with data of Okafor and Evers(1992) with results obtained from the simulation by Founargiotakis (2008). ....	47
Figure 3:10. Project Flow Chart.....	51
Figure 4:1. Comparison of simulations with and without 0.26 cutting volume- fraction .....	54
Figure 4:2. Goodness-of-fit graph for 2nd order polynomial response surface.....	56
Figure 4:3 Goodness-of-fit graph for Kringing response surface.....	56
Figure 4:4. Goodness-of-fit graph for Neural Network response surface.....	56
Figure 4:6. Kringing responce surface Input Parameter Sensitivity .....	58
Figure 4:7. Neural Network responce surface Input Parameter Sensitivity.....	58
Figure 4:8. Goodness-of-fit graph for 2nd order polynomial response surface.....	61
Figure 4:9. Goodness-of-fit graph for kringing response surface .....	61
Figure 4:10. Goodness-of-fit graph for Neural Network response surface.....	61
Figure 4:11. 2nd Order Polynomial Input Parameter Sensitivity .....	62
Figure 4:12. Kringing Input Parameter Sensitivity .....	63

Figure 4:13. Neural Network Input Parameter Sensitivity .....	63
Figure 4:14. 3D response chart of consistency index, Power-Law index and Pressure Gradient .....	64
Figure 4:15. 2D response chart of pressure gradient and cutting volume-fraction ( $\phi$ ) at 0.665m/s fluid inlet velocity. Fluid properties are: Yield Stress = 5.9, consistency index = 4.3, Power-Law index = 0.66. ....	65
Figure 4:16. 3D response chart for cutting concentration( $\phi$ ), and fluid inlet velocity( $v_{in}$ ). Fluid properties are the same as Figure 4:15. ....	66
Figure 4:17. 2D response chart of pressure gradient against drill pipe rotational velocity ( $\omega$ ). Fluid properties are identical to fluid used in Figure 4:3. ....	67

## LIST OF TABLES

Table 3:1. Experimental data sets to be modelled with hydrodynamic simulations..	38
Table 3:2. Summary of simulation parameters .....	41
Table 3:3. Parameters simulated from the data set from Founargiotakis's Study .....	45
Table 3:4. Comparison table of the results obtained by Founargiotakis and the simulation conducted for this study with the experimental results from Okafor and Evers .....	46
Table 3:5. Simulation Parameters .....	48
Table 3:6. Geometric data for annular flow simulations .....	48
Table 4:1. Pressure drop results by simulation with and without 0.26 cutting volume-fraction with the percentage of difference.....	53
Table 4:2.. Performance result of the responce surface types for drilling parameters study .....	55
Table 4:3. Performance result of the responce surface types for dimensionless number study .....	60

## **CHAPTER 1 : INTRODUCTION**

This chapter discusses the background of Managed Pressure Drilling (MPD) and the issues that are associated with it. The problem statement, objective and the scope of study are further discussed in detail within this chapter.

### **1.1 Background of Study**

In an ever increasingly cost sensitive environment, reducing the capital expenditure (CAPEX) is the ultimate goal for any drilling operations. The study of cutting transport is important as insufficient ability to transport and suspend drilled cuttings can lead to costly drilling problems. A formation at down hole conditions can be extremely heterogeneous, problem/ drilling issues may manifest in all forms and shapes at any time. Drilling through troubled zones in terms of hole cleaning can be tough but nevertheless a situation that needs to be overcome as the area of interest or target zones are of utmost priority for operators.

With the advent of directional drilling come endless possibilities in well trajectory control that were once thought to be unfeasible. One of the pioneering methods to directionally drill a well is by slide drilling and it has been practiced by the industry for more than 20 years. However, the industry realised the limitations of slide drilling and the irreplaceable advantages of rotary directional drilling in hole cleaning [1]. This distinct advantage has made extended-reach drilling (ERD) operations possible. Extended reach drilling has its own challenges however. Long horizontal sections synonymous with such drilling programs have unique hole cleaning problems, especially in ultra-deep ERD wells which are prone to high temperature and high pressure (HTHP) conditions. Such challenges are faced in the deep gas exploration campaign in the K-field of northern Oman. HTHP wells up to 4,800m true vertical depth subsea were plagued with issues such as low ROPs, tight holes, stuck pipes, and twist off [2]. Due to increasing well complexity, deteriorating drilling performance, escalating costs and non-productive time (NPT), deep gas exploration in the field have grown to become uneconomical without drilling optimization initiatives. A different approach was taken resulting in reduced drilling

time of 25 days, saving 1.25 million dollars per well in the process. Needless to say, the initiatives taken to optimize drilling were rewarding.

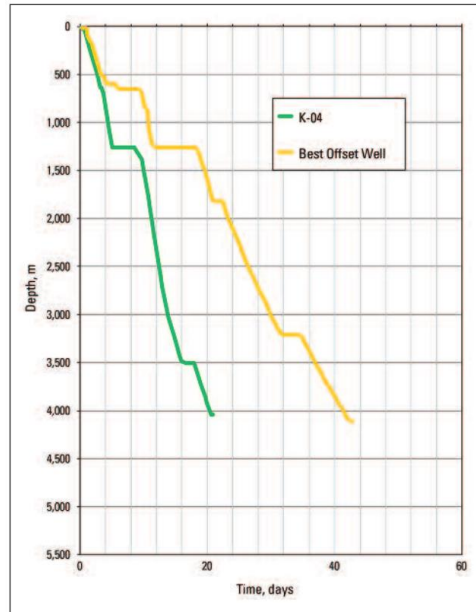


Figure 1:1. Time-depth curves for well K-04 in Northern Oman showing improvements compared to the previous offset well[2].

One such initiative was to ensure good hole cleaning. While it is believed that pipe rotation is a major factor that contributes to good hole cleaning in highly inclined wells [1], its effects are less known in HTHP environments. Drilling long horizontal wells allowed for much greater “pay zone” ( A reservoir or portion of a reservoir that contains economically producible hydrocarbons) penetration. It is no surprise that such well plans are increasingly popular. A side effect of these long horizontal sections is that drill pipes are essentially unsupported in the wellbore. Eccentricity occurs when the drill pipe rest on the lowside of the wellbore due to its own weight [3]. Despite the growing popularity of ERD, the effects of drillpipe rotation and eccentricity on cutting transport have not been fully exploited in horizontal HTHP environments. This project will address the shortcomings in pressure gradient prediction by simulation with non-Newtonian Yield Power law fluids.

## 1.2 Problem Statement

Having total control over the pressure in the annulus is the ideal scenario that is desired during MPD. In order to drill a well safely, well control is required where an overbalanced condition is achieved without fracturing the formation. This is achieved with good prediction of pressure gradient or losses in the annulus. Pressure gradient is defined as the pressure increase per unit of depth due to its density. Pressure gradient predictions, however, are not so straightforward. Cuttings, for example, will significantly alter the pressure gradient and the effect of this cannot be avoided. The pressure loss estimation across the well plays a considerable role in well control. Pressure drops can cause a shift in Equivalent Circulating Density(ECD) of the drilling fluid, creating an underbalanced condition and prompting a kick. A blowout can subsequently occur if well control measures have failed, leading to catastrophic incidents such as Deepwater Horizon.

No two fields can exhibit the same hydraulics. Heterogeneous conditions make it challenging to accurately determine the pressure gradient of a well. Accurate pressure loss prediction for non-Newtonian drilling fluids inside annulus is important to determine pump rates required and for selecting mud pump systems during drilling operations. A significant factor relating to hydrocarbon production is the cost, all wells if possible will be planned in such way to minimize cost. Increasing mud pressure and pump rates are significant sources of operating cost. This is an unfavorable situation for both Operator and Service provider, as the operators have to bear the increasing cost and the service providers risk liability when jobs are not completed within a specific timeframe due to drilling complications.

It is widely accepted eccentricity, cutting concentration, drillpipe rotation, and mud rheology affects the frictional pressure loss in the annulus. However, no explicit relation between the pressure gradient and the mud rheology with various drillings parameters has been made. This research aims to address the impact of eccentricity, inclination, drillpipe rotation, drilling fluid flow rate, mud rheology, and cuttings on the pressure gradient in the annulus.

### 1.3 Objectives

The research objectives are as follows:

- To simulate the effects of **eccentricity, drillpipe rotation, inclination, cutting concentration through volume fraction, and mud rheology** on the pressure gradient in the annulus.
- To analyze the simulation result and suggest new or improved regression model for pressure gradient.

### 1.4 Scope of study

This study covers the following:

- The drilling mud is to be considered as non-Newtonian yield power law fluid governed by shear stress – shear strain relations proposed by Hemphill et al (1993).
- Effects of drill pipe rotation, inclination, cutting concentration and mud rheology, and flow rate are investigated.
- Effects of temperature and pressure exerted by the wellbore are not to be considered.
- The number and location of design points for the simulation will be decided based on Design of Experiment (DOE). And, the planned regression models for the pressure gradient will be developed assuming polynomial functions in the context of non-dimensional parameters.



## CHAPTER 2 : LITERATURE REVIEW

### 2.1 Introduction

Drilling for oil and gas has come a long way since the first oil wells, called “wildcats,” were drilled to shallow depths of approximately 1000 feet. Hole depth was limited because of primitive drilling equipment and the limited technology. Fast forward to the 1900s and the drilling techniques were vastly improved with the use of rotary rigs which permitted greater drilling depths. Nonetheless, drilling was still limited to vertical wells, limiting the amount of reservoirs accessible at the time. The history of drilling period can be separated into three distinct periods. First there is the early period ranging from ancient times up to completion of the spindle top well in 1901, admittedly the first commercially important oil well produced by rotary process. Second there is the period from 1901 to 1928, when engineers were conducting test on the drilling muds to meet specific drilling needs and the third extend from 1928 to present. The first era was an experiment. The second was of practice and the third is of science[4].

Only plain water was used as drilling fluids initially. It wasn't until 1880's when Chapman came up with the idea of using streams of water and quantity of plastic material to form an impervious wall along the well bore and this was the beginning of science of mud engineering. When the advantages of drilling fluids were recognized, they became an essential part of the planned drilling program. At first, the mud was used primarily to clean, cool and lubricate the bit as it drilled through formations. Its use grew as drilling demands became more challenging with deeper and deeper wells drilled. Today, drilling fluids is used to prevent well-control issues, minimize formation damage and provide valuable information about the wellbore. The fluid also removed the formation cuttings from the hole by circulating the mud using surface pumps, which is essential for hole cleaning.

The circulation of drilling fluids has become an important part of every drilling operation. For vertical or near-vertical drilling, the problems related to insufficient cutting transport appears to have been adequately contained. In drilling directional wells, however, the inclined annulus poses several problems not encountered in vertical wells. Cutting concentrations increase drastically from an inclination of 20°

and above. It was noted that at these critical angles of  $30 < \theta < 60^\circ$ , the cutting bed usually was sliding downward against the flow, resulting in a very high cuttings concentration[3]

This is reflected in a full-scale experiment conducted by Sifferman [5] where a cutting bed formation and sliding differed at certain inclinations within the critical range. At hole angles of  $60^\circ$  and higher, the bed appeared to be well-packed, while at  $45^\circ$  it was considerably fluidized. He described the cuttings-bed height as varied over the axial length of the viewing sections. This generally occurred at hole angles of  $45$  and  $60^\circ$ , where there was a dynamic bed that varied locally with time. At  $45^\circ$ , the bed continuously slid down along the casing wall. This caused variations in local bed heights, especially at the lower-mud velocities. Such sliding behavior was not as prevalent at higher inclinations.

At near horizontal to horizontal inclinations of  $60 < \theta < 90^\circ$ , both Sifferman and Tomren agree that a cutting bed would be formed on the low side of the hole [3, 5]. It was noted that bed formation was almost instantaneous at these high angles of inclination. The bed did not slide downward and was stagnant with or without flow.

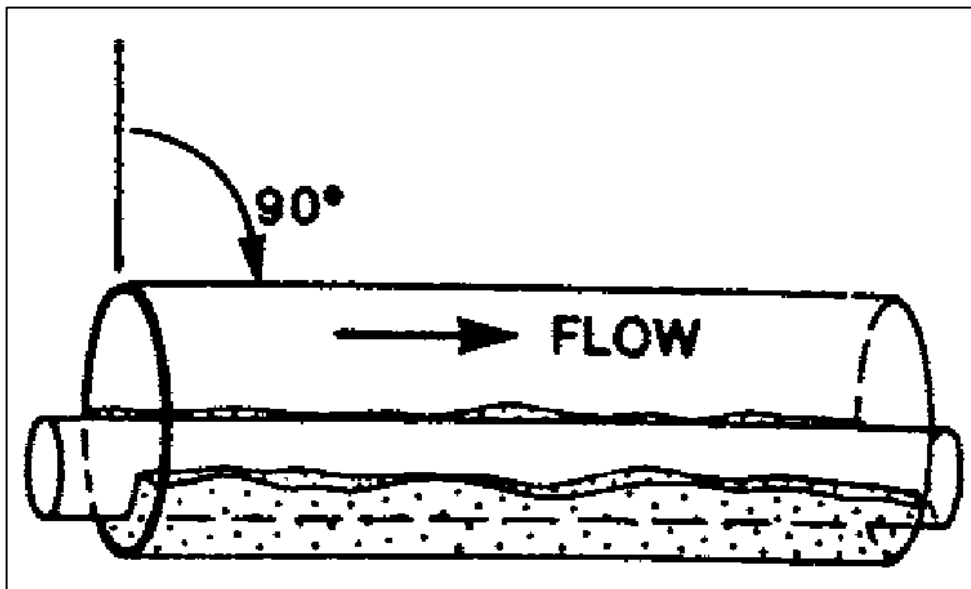


Figure 2:1 Illustration of cutting bed formation at a horizontal inclination of  $90^\circ$  by Sifferman [5].

Drill pipe rotation has a significant effect on hole cleaning and the reduction in the cutting weight in the annulus due to this rotation can be as high as 80 percent[6]. It was also found in Sanchez's study that at 90 degrees from vertical and

low flow rates, high rotary speeds produce the most benefits. The opposite is true at high flow rates. In lower inclinations no critical range of rotary speeds was identified but higher meant better. Pipe rotation also improves bed erosion once drilling has stopped. Both the residual concentration and the erosion time are reduced and the motion of the drillpipe determines the contribution of pipe rotation to hole cleaning. Orbital motion is needed for significant improvement to occur.

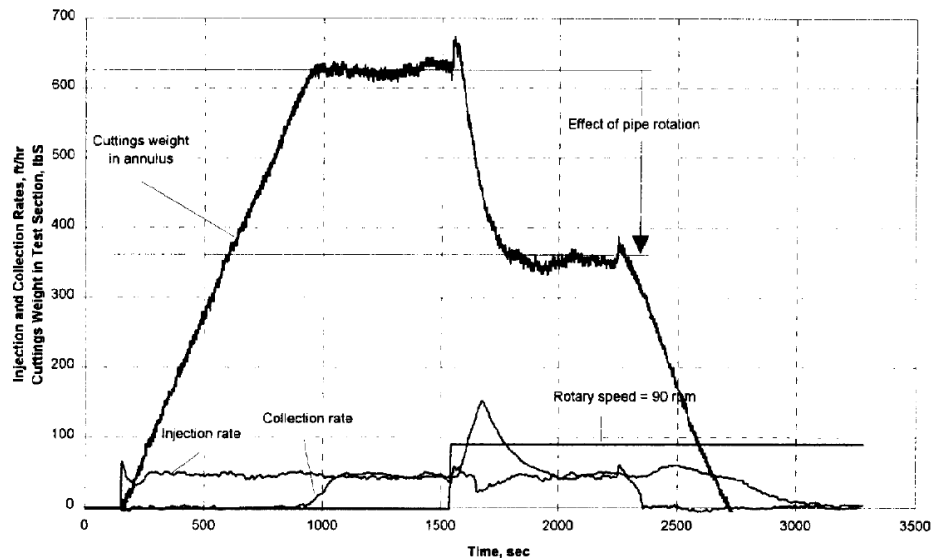


Figure 2:2. Graph depicting the prominent effect of drill pipe rotation on cutting removal by Sanchez [6].

In vertical holes, cuttings behaviour was nearly the same for all eccentricities. The only difference was the noticeable reduction in cuttings velocity in the reduced annulus area of the eccentric annulus [3].

For the inclined annulus, however, it was observed that cuttings build up was lowest when the inner pipe was concentric with the outer pipe. The rate of bed build up appeared to be slightly faster with the positive-eccentricity case. The axial propagation of the bed also appeared to be slowest at this eccentricity.

In another test conducted by Tomren, it was found that the effects of liquid viscosity on cuttings behavior depended on the flow regime. His report noted that in laminar flow, bed formation in high viscosity fluids was slow compared to that in low-viscosity fluids. A smaller bed eventually was formed in the high viscosity fluid. In turbulent flow, however, although a slightly smaller bed of cuttings did form in the higher viscosity fluid, bed formation was equally fast for both cases [3]. He concludes that this phenomenon may be related to particle-slip velocities, which are

greater in turbulent flow than in laminar flow. Also, particle slippage is independent of viscosity in turbulent flow.

For low angles of inclination, a bed of cuttings was formed at low liquid velocities ( $< 0.61$  m/s). This bed was generally small and unstable, especially in turbulent flow with rotating inner pipe [3, 6]. At higher liquid velocities ( $>0.91$ m/s), neither a steady bed nor severe slugging occurred. The cuttings were transported smoothly at the low side of the annulus. This is generally reflected at higher inclinations where velocities higher than 0.91 m/s would exhibit significantly less or no cutting beds.

## **2.2 Drilling Fluids**

### **2.2.1 Drilling Fluid Functions**

Although removing cuttings from the well and controlling formation pressures are the primary and the most important functions of the drilling fluid on every well, now mud serves several other important functions in modern drilling operations. Some may not be essential on every well and the order of importance is determined by well conditions and ongoing operations. The most common drilling fluid functions are [7]:

- i. Removal of cuttings
- ii. Control formation pressures
- iii. Suspend and release cuttings
- iv. Maintain well bore stability
- v. Minimize reservoir damage
- vi. Cool, lubricate, and support the bit and drilling assembly
- vii. Transmit hydraulic energy to tools and bit
- viii. Ensure adequate formation evaluation
- ix. Control corrosion
- x. Facilitate cementing and completion
- xi. Minimize impact on the environment
- xii. Enable data transmission by mud pulse telemetry

Different mud properties may affect a particular function. Hence Mud properties should be recognized for their influence on all functions and the relative importance of each function.

### **2.2.2 Drilling Fluid Properties**

The mathematical relationship between shear rate and shear stress describes the behavior of the fluid, flow and deformation, and hence defines the Rheological Model of the fluid. The use of those rheological models requires measurements of shear stress at minimum two or more shear rates, then from those measurements, the shear stress at any other shear rate can be calculated [7].

The fluids represented with a linear relationship, i.e., if the shear-stress is doubled then the shear-rate will also double or in other words, if the circulation rate is doubled then the pressure required to pump the fluid will double, then those fluids are known as "Newtonian fluids". The viscosity of such fluids remains constant with changing shear rate.

Most drilling fluids are not Newtonian. What this means is the shear stress is not directly proportional to shear rate. Such fluids are called "Non-Newtonian". The viscosity varies with changing shear rate. To be meaningful, a viscosity measurement made on a non-Newtonian fluid must always specify the shear rate. The term "effective viscosity" is used to differentiate viscosity measurements made on non-Newtonian fluids from Newtonian fluids. Non-Newtonian fluids can be classified as shear-thickening, shear-thinning, and visco-plastic [8].

A shear-thickening fluid is defined as a fluid in which apparent viscosity increases with the increase of shear strain rate. Fluids which display such characteristics are also called dilatant fluids. A shear-thinning fluid is the opposite of shear-thickening fluid where apparent viscosity decreases with the increase of the rate of shear strain which is also called as pseudoplastic fluid [9].

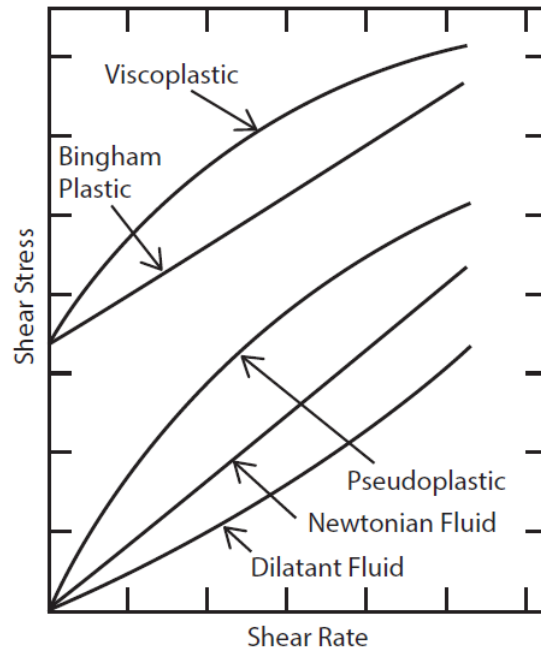


Figure 2:3. Characteristics of different non-Newtonian fluids [9].

When sheared, a typical non-Newtonian fluid will exhibit flow behavior similar to that shown in the figure below.

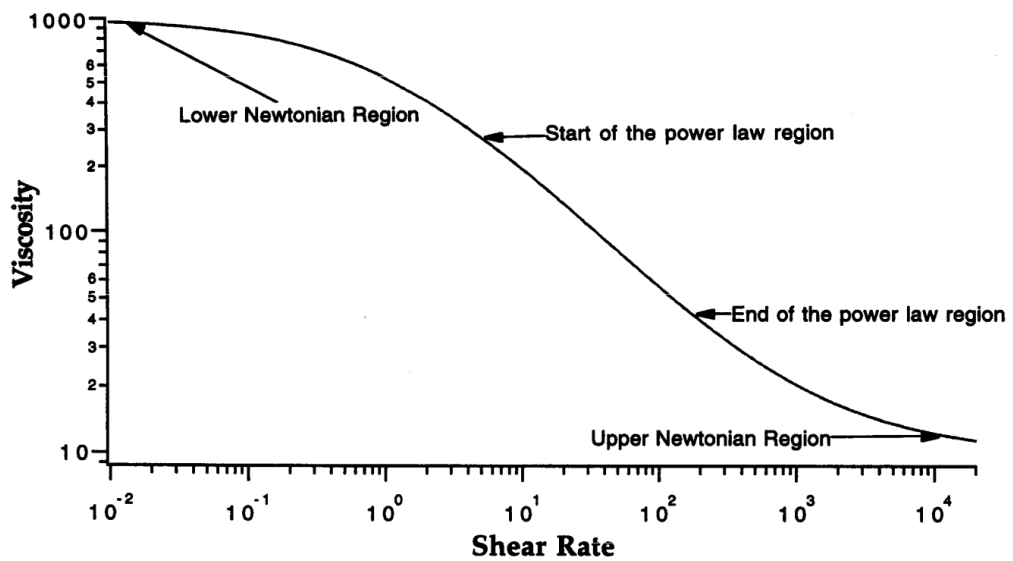


Figure 2:4. Typical non-Newtonian fluid viscosity versus shear rate behaviour [7]

The fluid first gives a Newtonian response (lower Newtonian region) to the shear rate and then transition into a power law region. When the shear rate gets high enough a second transition occurs to Newtonian behaviour (upper Newtonian region). The rheological behavior of drilling muds fall into two broad classes,

namely Bingham plastic and power law. Bingham Plastic model can be generalized to Herschel-Bulkley. This will be discussed in the following section.

Non-Newtonian fluids in many instances exhibit viscoelasticity. There has been some speculation that viscoelasticity is an important property, but there is little or no proof that it is. Viscoelastic effects will not be discussed in this project.

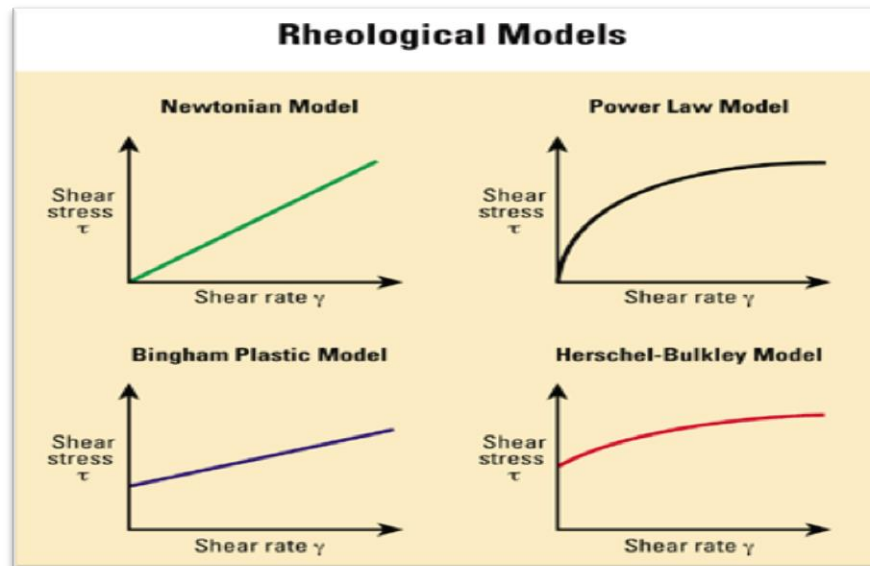


Figure 2:5. General Fluid Rheological Model

### 2.2.3 Power Law Model

The Power-law Model is also known as the Ostwald-de Waele model. It is considered as a generalized Newtonian fluid. With increased use of polymer-based fluids in the oil field, the power law (PL) Theological model became popular because it fits the behavior of these fluids better than the Bingham plastic model [10]. The two key terms in the Power Law model are the consistency index (K) and the fluid flow index (n).The power law is defined as:

$$\tau = K\dot{\gamma}^n \tag{2.1}$$

This mathematical relationship is useful due to its easiness, but only approximately describes the behavior of a real non-Newtonian fluid. Theoretically, the major

stumbling block to modeling of the power law is the fact that most drilling fluids have a yield stress, something for which this model cannot account. The net result is that in hydraulics equations, PL modeling underpredicts both annular pressure losses and ECDs [10]. This model can be subdivided into three different types of fluids based on the value of their flow behavior index which are dilatants fluid ( $n>1$ ), pseudo plastic fluid ( $n<1$ ) and Newtonian fluid ( $n=1$ ). The power law is only valid for laminar flow regime: thus low shear rate.

#### 2.2.4 Bingham plastic model

The shear stress-shear rate is a linear relationship and slope represents the Bingham plastic. The Bingham plastic model calculates two parameters: yield point (YP) and plastic viscosity (PV) [10]. The intercept is the yield stress of the fluid. Therefore, a minimum pressure is required to overcome the yield stress to initiate flow [11]. The model is given as

$$\tau = \tau_y + \mu_p \dot{\gamma} \quad (2.2)$$

The Bingham plastic model is the typical viscosity model used which can fit high shear rate viscosity data reasonably well.  $\mu_p$  (plastic viscosity) is generally associated viscosity of base fluid, size and shape of solids in slurry. The yield stress is associated with tendency of the components to build a shear resistant. While the Bingham plastic model simulates fluid behavior in the higher shear rate range (300-600 rpm), it usually fails in the low shear rate range, which is the area of interest for simulating annular flow behavior. Shear stresses measured at high shear rates usually are poor indicators of fluid behavior at low shear rates [10].

#### 2.2.5 Hershel Buckley model

The study from Hemphill [10] stated that Hershel Buckley model is favored as an alternative to Power law and Bingham plastic model due to its more accurate result of the rheological model. It merges the theoretical and practical aspects of Bingham plastic and PL models. The model is expressed as:

$$\tau = \tau_y + K \dot{\gamma}^n \quad (2.3)$$



The key terms are the yield point ( $\tau_y$ ), consistency index (K), and n is the exponent, referred to as power-law index. In theory this yield stress is identical to the Bingham plastic yield point, though its calculated value is different. The model works well for water-based and oil-based drilling fluids because both exhibit shear-thinning behavior and have a shear stress at zero shear rate.

Research done by Kelessidis et al, (2006) claim the results outcomes have proven that it is vital to create the best simulation of rheological behavior of drilling fluids before computing hydraulics parameters. This will eventually help to encounter the problems during drilling operation of existing drilling fluids.

### 2.2.7 Foam with Quality

Foam has its importance in drilling due to its high cutting-carrying capacity compared to many conventional fluids [1]. The typical applications of foam include underbalance or near-balanced drilling where it has enabled successful exploitation of low-pressure, low-permeability, or naturally fractured reservoirs. This is due to its nature of being an insulator for circulation problems. However, there is no expression to the foam model but is typically dependent on foam quality. Foam quality, given the liquid flow rate,  $Q_L$  and the gas flow rate at standard condition,  $Q_{g,s}$ , can be expressed as:

$$\Gamma = \frac{1}{1 + \frac{Q_L}{\left\{ \frac{\rho_{g,s} Q_{g,s}}{M_g} - Q_L P K_{H,T_s} \exp \left[ c \left( \frac{1}{T} - \frac{1}{T_s} \right) \right] \right\} \frac{R_g T}{P}}} \quad (2.1)$$

where

$\rho_{g,s}$  = gas density at standard conditions

$M_g$  = molar mass (kg/mole) of the gas

$R_g$  = the universal gas constant (8.314 J/mol.K)

P and T = absolute pressure (Pa) and Temperature (Kevin)

Foam and mud have vastly different rheological properties and Duan believes it should have substantial effect on hole cleaning as his findings conclude that pipe

rotation significantly reduces cutting concentration in a horizontal annulus during foam drilling as well as reduces a considerable amount of frictional pressure loss.

The reduction in cutting concentration was found to be up to 40% at medium foam velocity (3ft/sec) when pipe is rotated at 120RPM. The decrease in frictional pressure loss is up to 50% at medium foam velocity and is more than 60% at a low velocity. Improvement in hole cleaning by increasing foam velocity is limited when low-to-medium quality foams are used. He adds that an increase in foam velocity noticeably decreases cutting concentration with high-quality (0.9) foam. This comes with a drawback however. Increasing foam quality causes a significant increase in frictional pressure loss. Rotating the drillpipe does at least help to minimize the increase in pressure loss caused by an increase in foam velocity.

He ends his report by concluding that pipe rotation in the range of 80 to 160 RPM and a foam superficial velocity higher than 5 ft/sec is highly recommended during foam drilling. Foam quality lower than 0.7 is not recommended for drilling application in a horizontal well.

### **2.3 Computational Fluid Dynamics (CFD)**

Computational Fluid Dynamics (CFD) is emerging as a very promising tool in modeling hydrodynamics. Simulations from CFD are used to evaluate drilling parameters and performances to help aid drilling optimization. This evaluation is used to determine the optimum set of parameters for improved cutting transport and frictional pressure loss. The results were certified to varying degrees using experiments [1]. Navier-Stokes fluid dynamic equation is solved using CFD software with a numerical method. Often used as an alternative or a complement to experimental testing, this technique can rapidly and frugally produce a large amount of information about a flow and is particularly attractive when the conditions are difficult to replicate experimentally.

### **2.3.1 CFD Applied to Cutting Transport Predictions**

As cutting transported by mud is a simultaneous flow of materials with different states or phases, it is considered a multi-phase flow. The term multiphase flow is used to refer to any fluid flow consisting of more than one phase or component [12]. It was noted that a persistent theme throughout the study of multiphase flows is the need to model and predict the detailed behavior of those flows and the resultant manifested phenomena [12]. With the recent increased computational capabilities available, CFD is a promising tool in modeling hydrodynamics [10].

Duan [1] conducted an experimental study and modeling of cutting transport using foam with drillpipe rotation. A mechanistic model and associated computer simulator was developed for practical and field application. Model used to predict cutting concentration, bed height and pressure drop during horizontal foam drilling. Comparison between model predictions and various experimental data sources show that the difference is less than 15% in most cases.

In a study conducted by Ekambara [13] titled “Hydrodynamic Simulation of Horizontal Slurry Pipeline Flow Using ANSYS-CFX”, the behavior of a horizontal solid-liquid (slurry) pipeline flows was predicted using a transient three-dimensional hydrodynamic model based on the kinetic theory of granular flows. The simulation result was compared with a number of experimental work from other studies. The effect of in situ solids volume concentration, particle size, mixture velocity, and pipe diameter on solid concentration profiles, particle and liquid velocity profiles, and frictional pressure loss were investigated. The simulation results corresponded to the experimental data well. Ekambara [13] however had different applications for this simulation such as long-distance transport of materials like coal, and mineral ore. The behavior of these materials when transported through a horizontal pipeline however is similar to cutting transport while drilling.

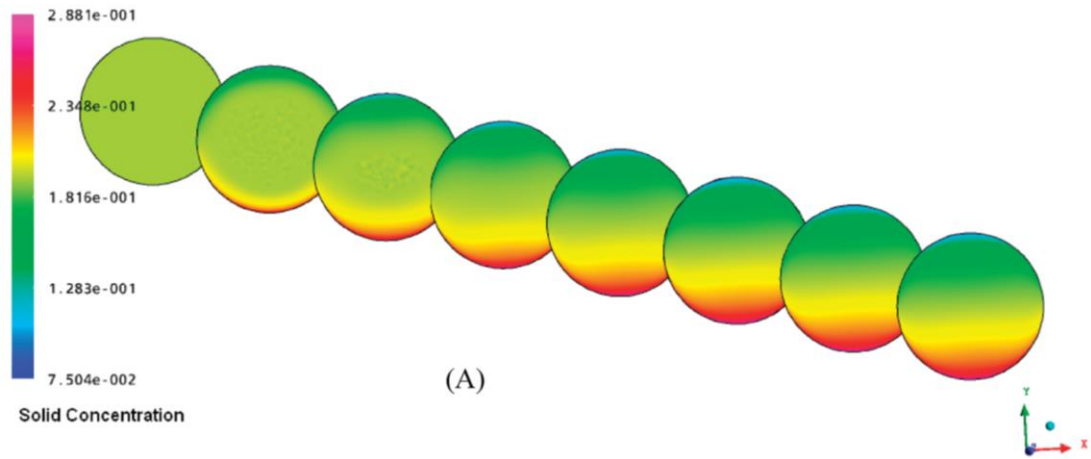


Figure 2:6. Contour plots for particle concentration taken at regularly spaced axial positions over the 10m control volume. The following conditions were simulated: cutting diameter 90  $\mu\text{m}$ , and liquid velocity 3.0 m/s.

The findings from Ekembara [13] show that even with liquid flowing at high velocity, a settled bed of solids were formed over the 10m control volume of his simulation. This is reflected in the experimental study by Tomren and Sanchez [3, 6] where cuttings would settle and form a bed in a horizontal annulus. The application of this model to horizontal cutting transport will be highly suitable due to the similar parameters of study. This study will be used as a benchmark for sensitivity analysis.

In a separate study by GhasemiKafrudi [14], CFD was used to great effect. An in-house code developed to calculate velocity and pressure fields from the simulations conducted.

Mud velocity profile using Herschel-Bulkley model and solid phase volume fraction was locally calculated with pressure drop though the annulus also taken into consideration. His findings showed that drilling fluid with high yield exhibited bigger pressure drop. Pressure drop also increased by enhancing drillstring rotation. Maximum calculation error of 18% though friction factor calculation. This study however only considered vertical or near-vertical conditions in 0.311m hole size. This is not under slim hole conditions but the study serves as a guideline to set expectations from this project. As the study fail to take into consideration the eccentricity, this is an area of interest that can be further exploited.

## **2.4 Pressure Loss Predictions**

Various studies had been conducted on the pressure loss through annulus during drilling operations. A notable study by Rooki [8] utilizes Artificial Neural Network to estimate the pressure loss of Herschel-Bulkley drilling fluids in horizontal annulus to great effect. The diameter ratio, eccentricity, flowrate and rheology was used as inputs to the response surface with 5% average relative error for the prediction of pressure loss when compared to experimental results.

Pilehvari similarly attempted to generalize hydraulic calculations but instead used Rational Polynomial Model [15]. The model is capable of accurately representing rheogram of virtually any time-independent fluid. The prediction of models was compared to published experimental data with high accuracy obtained with just a small number of adjusted parameters. The studied cases include laminar and turbulent flow for varying drilling fluid in concentric fluid. While the model was capable of predicting pipe and annular flow pressure drop in laminar and turbulent region, effects of other important drilling parameters such as eccentricity, inclination, and cuttings were not taken into account. Pilehvari claims that the model is suited for correlating equation in general computer program for hydraulic calculation [15].

## **2.5 Borehole Temperature and Pressure**

The temperature and pressure of the borehole environment is another critical factor that may influence the hole cleaning efficiency of drilling mud due to significant change in the rheological properties of drilling mud [16]. In Alderman's study, it was found that the high-shear viscosity of drilling fluids decreases with increasing temperature and increases with pressure to an extent which depends on mud density. The behavior of these fluids is largely governed by the viscosity and compressibility characteristics of the continuous phase. The yield stress of the tested mud is essentially independent of pressure for the fluids studied and only weakly dependent on temperature below a temperature which is characteristic of the specific particle interactions within the mud. Above the specific temperature, the yield stress

increases rapidly with temperature. These changes in the rheological properties of drilling fluids play a monumental role in cutting transport [17].

As for drilling with foam, Duan [1] determined that the effects of downhole pressure and temperature on cutting concentration and pressure drop. Tendencies noticed is increasing pressure causes a slight decrease in cutting concentration. However, the frictional pressure drop increases with pressure.

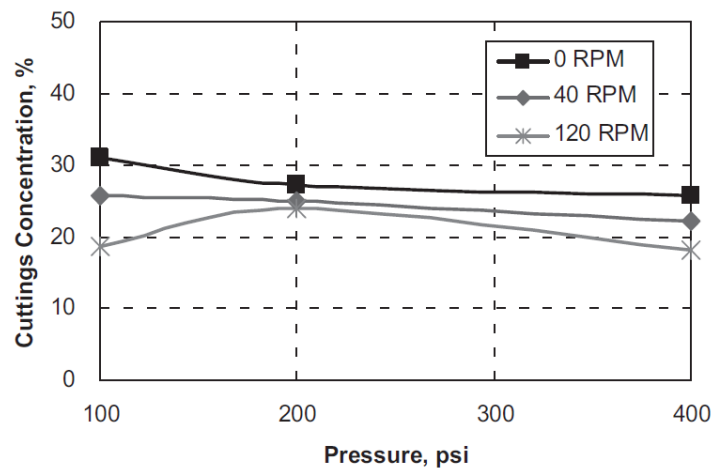


Figure 2:7. Cutting concentration vs. downhole pressure for 0.8-quality foam with pipe rotation [1].

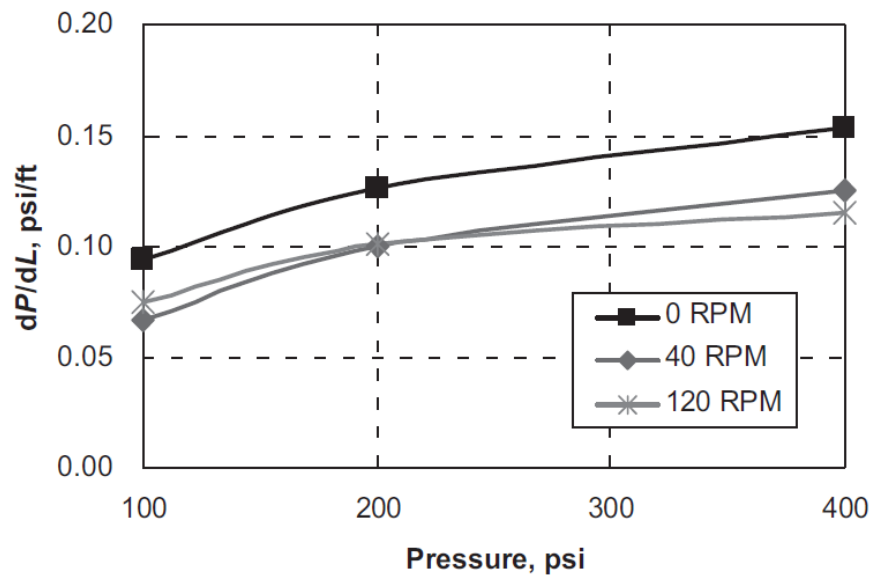


Figure 2:8. Pressure drop vs. downhole pressure for 0.8-quality foam with pipe rotation [1].

In the same study, Duan noted the effects of downhole temperature whereby a higher temperature generally results in a higher cuttings concentration. The frictional pressure drop decreases with an increase in temperature.

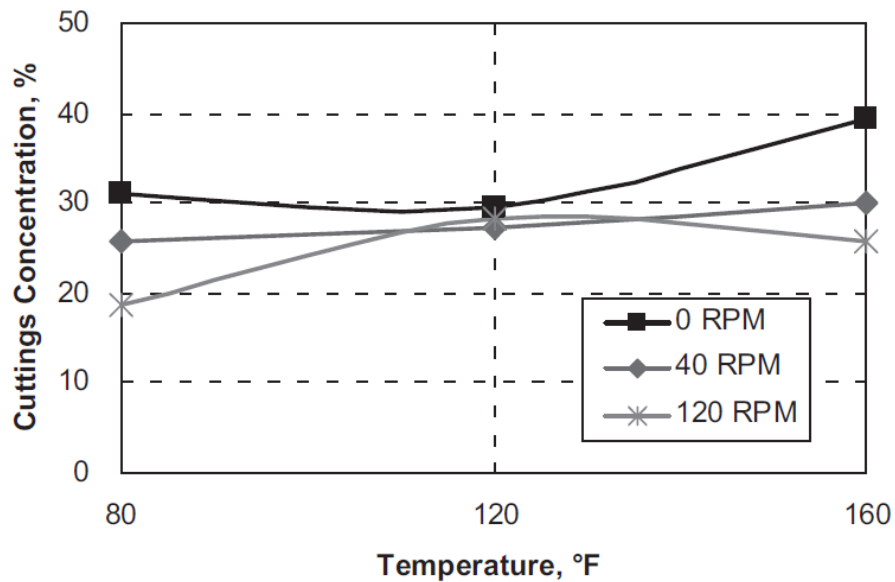


Figure 2:9. Cutting concentration vs. downhole temperature for 0.8-quality foam with pipe rotation [1]

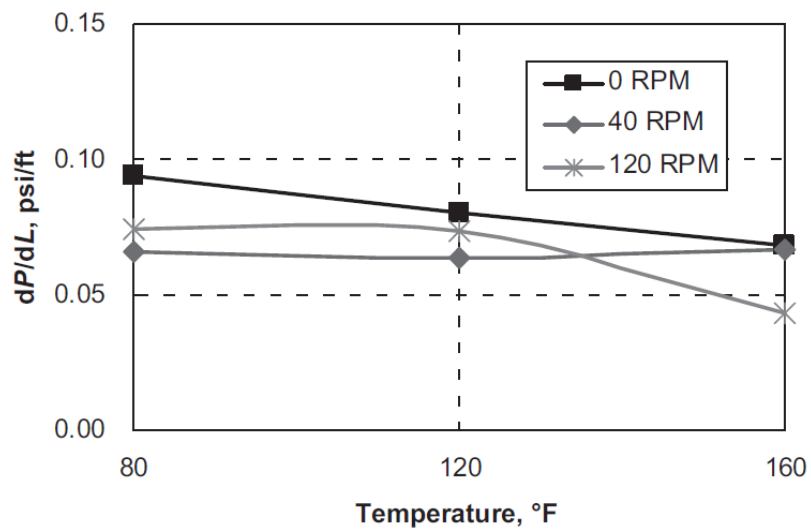


Figure 2:10. Pressure drop vs. downhole temperature for 0.8-quality foam with pipe rotation [1].

Therefore, bottomhole temperature is considered as one of the critical parameters in simulating the hole cleaning efficiency and pressure gradient of drilling mud and foam.

## 2.6 Summary

Drilling fluids play a major role in cutting removal. Its function of maintaining wellbore stability and cutting transport has been well understood. The increase in cutting concentration causes a positive pressure gradient change. When the increase in pressure becomes too substantial, the formation can potentially be fractured unintentionally. Another major impact drilling fluid and its rheological properties causes is the pressure drop through the annulus. Drilling mud with high yield stress has shown to cause more pressure drop through the annulus. Consensus was also made that drill string rotation causes pressure drops which can affect wellbore stability. The eccentricity effect on the pressure gradient is an area which is relatively unexplored.

Computational fluid dynamics has been universally accepted as a tool which can accurately mimic experimental results given certain parameter calibrations. Sensitivity analysis in both studies from Duan and GhasemiKafrudi showed agreeable results compared to the experimental studied that they are based on [1, 14]. CFD is a powerful tool that is able to help answer some of the unstudied drilling conditions.

- The effect of mud rheology
- Cutting
- Inclination
- Pressure gradient
- Mud flow rate
- Eccentricity

There are no studies conducted which effectively relates the effect of these parameters on the pressure gradient in the annulus and the effect of high temperature and pressure. The next alternative is the study carried out by Duan in 2010, which only covers foam drilling. Yield Power Law model will be used. It is necessary to use more powerful rheological models and more rigorous calculation when drilling in deep, slim or horizontal onshore or offshore wells.



## CHAPTER 3 : METHODOLOGY

### 3.1 Introduction

Each phase of the project can be broken down into four major task that can be idealized as four blocks arranged sequentially, Figure 3.1. The first part determines the drilling parameters to be modeled. This step includes mud rheology characterization and borehole as well as operating conditions. The second involves generating a model and subsequently, a good quality mesh is generated. Once the overall mesh is acquired, simulations based on the predetermined operating conditions are run.

Once the overall method is acknowledged, realization of each block is possible through details planning. In this regards, a suitable flowchart is developed as portrayed in Figure 3.2. The corresponding Gantt chart is as shown in Figure 3.3.

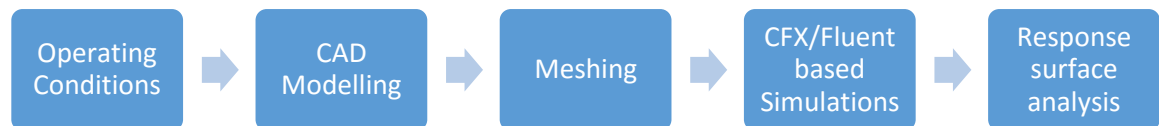


Figure 3:1. Sequential task blocks

#### 3.1.1 Literature Review

The research will be focusing on drillpipe rotation, mud flow rate and rheology, cutting concentration, inclination, and eccentricity on cutting transport under Yield Power Law effect in the annulus. To be more specific, an implicit correlation between these parameters will be developed and subsequently an attempt to create an explicit formula will be conducted. The suitable parametric model for the various parameters for pressure gradient predictions will be determined.

Information on drilling parameters will be gathered to study and improve prediction. Fluid rheology, geometry of a varied inclination wellbore, CFD simulation studies, and drilling parameter effects on cutting transport are studied as the main point in this study.

### **3.1.3 CFD modeling and simulation**

The authenticity and strength of the project relies on this technique where simulation and modeling the cutting transport under determined conditions. The initial benchmark CFD model used in this work is based on the extended two-phase model, which uses granular kinetic theory to describe particle-particle interactions. Particles are considered to be smooth, spherical, inelastic, and to undergo binary collisions. The fundamental equations of mass, momentum, and energy conservation are then solved for each phase. Appropriate constitutive equations have to be specified in order to describe the physical and/or rheological properties of each phase and to close the conservation equations. Subsequent benchmark CFD models utilized only a single-phase laminar flow model with cuttings introduced as a fluid viscosity and density modifier.

### **3.1.4 Documentation**

The findings and results as well as the literature review were document throughout the study.

## **3.2 Transient and Laminar Hydraulic Model for Managed Pressure Drilling**

Fundamental equation regarding Yield Power Law is analysed. Base case setting is carefully reviewed and selected to be used as comparison of evidence that the constructed model can be authorized. Some basic engineering assumptions are required to determine the flow of non-Newtonian Yield Power-law fluids through annulus.

### 3.2.1 Fundamental equation and theory

Fundamental equation regarding Yield Power Law is analysed. Base case setting is carefully reviewed and selected to be used as comparison of evidence that the constructed model can be authorized. Some basic engineering assumptions are required to determine the flow of non-Newtonian Yield Power-law fluids through annulus. As drilling fluids will be used as the material flowing in the annulus domain, a rheological model which describes the relation between shear stress and shear rate is needed. The Herschel-Bulkley fluid rheological model, defined by equation 2.3 in the literature review will be used.

Continuity and momentum are the core conservation equations that will be solved with ANSYS CFX. The phase is described using incompressible, volume-averaged, transient Navier-Stokes equations. The momentum balance for the liquid phase is given by the Navier-Stokes equation, modified to include an interphase momentum transfer term:

$$\frac{\partial}{\partial t}(\rho_1 \alpha_1 \mathbf{u}_1) + \nabla \cdot (\rho_1 \alpha_1 \mathbf{u}_1 \mathbf{u}_1) = -\alpha_1 \nabla p + \rho_1 \alpha_1 \mathbf{g} + \nabla \cdot \boldsymbol{\tau}_1 + \mathbf{F}_{km} \quad (3.1)$$

where  $\alpha$  is the concentration of each phase,  $\mathbf{u}$  is the velocity vector,  $\rho$  is the density,  $\mathbf{g}$  is the acceleration of gravity,  $p$  is the thermodynamic pressure,  $F_{km}$  is the sum of the interfacial forces (including the drag force  $F_D$ , the lift force  $F_L$ , the virtual mass force  $F_{vm}$ , the wall lubrication force  $F_{WL}$  and the turbulent dispersion force  $F_{TD}$ ).

The representation of the liquid-phase stress tensor,  $\boldsymbol{\tau}_1$ , is given as:

$$\boldsymbol{\tau}_1 = \mu_1 [\nabla \mathbf{u}_1 + (\nabla \mathbf{u}_1)^T] - \frac{2}{3} \mu_1 (\nabla \cdot \mathbf{u}_1) \mathbf{I} \quad (3.2)$$

The solid phase momentum balance is represented as:

$$\frac{\partial}{\partial t}(\rho_s \alpha_s \mathbf{u}_s) + \nabla \cdot (\rho_s \alpha_s \mathbf{u}_s \mathbf{u}_s) = -\alpha_s \nabla p + \rho_s \alpha_s \mathbf{g} + \nabla \cdot \boldsymbol{\tau}_s + \mathbf{F}_{km} \quad (3.3)$$

The solids stress tensor,  $\boldsymbol{\tau}_s$ , can be expressed in terms of the solids pressure,  $P_s$ , bulk solids viscosity,  $\zeta_s$ , and shear solids viscosity,  $\mu_s$ :

$$\boldsymbol{\tau}_s = (-P_s + \zeta_s \nabla \cdot \mathbf{u}_s) \mathbf{I} + \mu_s \left\{ [\nabla \mathbf{u}_s + (\nabla \mathbf{u}_s)^T] - \frac{2}{3} (\nabla \cdot \mathbf{u}_s) \mathbf{I} \right\} \quad (3.4)$$

Kinetic Theory of Granular Flow is applied to the benchmark problem involving cutting simulations. In these models, the constitutive elements of the solids stress are functions of the solids phase granular temperature,  $\Theta_s$ , defined to be proportional to the mean square fluctuating particle velocity resulting from interparticle collisions:  $\Theta_s = u'_s{}^2/3$ , where  $u'_s$  is the solids fluctuating velocity. The granular temperature is determined from a transport equation. The conservation of the solids fluctuating energy balance can be written as:

$$\frac{3}{2} \left[ \frac{\partial}{\partial t} (\alpha_s \rho_s \Theta_s) + \nabla \cdot (\alpha_s \rho_s \mathbf{u}_s \Theta_s) \right] = \tau_s : \nabla \mathbf{u}_s + \nabla \cdot (k_s \nabla \Theta) - \gamma_s + \Omega_{ls} \quad (7) \quad (3.5)$$

The left-hand side of this equation represents the net change of fluctuating energy. The first term on the right-hand side represents the fluctuating energy due to solids pressure and viscous forces. The second term is the diffusion of fluctuating energy in the solids phase. The third term,  $\gamma_s$ , represents the dissipation of fluctuating energy and  $\Omega_{ls}$  is the exchange of fluctuating energy between the liquid and solids phase.

Introducing cuttings into the drilling fluid as a function of volume-fraction does not change the fluid's rheological properties. It does, however, change the fluid's density and viscosity [18, 19].

The relative viscosity is calculated with the following equation [18]:

$$\frac{\mu_s}{\mu_0} = 1 + 2.5\varphi + 10.05\varphi^2 + A \exp(B\varphi) \quad [18], \quad (3.6)$$

where  $\varphi$  is the dimensionless cutting volume-fraction and  $\frac{\mu_s}{\mu_0}$  is the mean value of relative viscosity. The coefficients A and B are 0.00273 and 16.6.

The density with cutting volume-fraction is given as [19]:

$$\rho = \varphi \rho_s + (1 - \varphi) \rho_L \quad (3.7)$$

where  $\rho_s$  is the density of the solid cuttings, and  $\rho_L$  is the density of the liquid.

Friction factor calculations require Reynolds, Froude, Taylor and Bingham dimensionless number. The effect of each of this dimensionless numbers on the pressure gradient in annulus will therefore be investigated.

The effective Reynolds number for a non-Newtonian fluid such as mud can be calculated with [20]:

$$Re_{eff} = \frac{\rho V d_h}{\mu_{eff}} \quad (3.8)$$

where  $d_h$  is the hydraulic diameter. For flow in annulus,  $d_h = \text{hole size} - \text{drill pipe outer diameter}$ .

The effective shear rate is tabulated with:

$$\dot{\gamma}^2 = \left(\frac{V}{d_h}\right)^2 + \left(\frac{\omega R_{in}}{d_h}\right)^2 \quad (3.9)$$

The Taylor Number is defined as follows [21]:

$$Ta = \left(\frac{\rho \omega}{\mu_{eff}}\right)^2 R_{out}(R_{out} - R_{in}) \quad (3.10)$$

where  $R_{in}$  and  $R_{out}$  is the radius of the internal (drill pipe) and external pipe (wellbore).

Herschel-Bulkley fluids can also be characterized by Bingham number and is defined as follows [22]:

$$Bi = \frac{\tau_y}{K} \left(\frac{d_h}{V}\right)^n \quad (3.11)$$

Ozbayoglu's work [23] determined that Froude dimensionless parameter should be considered in friction factor determination. It is defined as:

$$Fr = \frac{V}{\sqrt{g d_h}} \quad (3.12)$$

### 3.2.1 Benchmark Problem by Ekembara

The initial benchmark problem simulated is by Ekembara [13]. In his study, ANSYS-CFX was used for simulation. Behavior of slurry pipeline flow was predicted using transient 3D hydrodynamics model based in kinetic theory of granular flow. The model is relevant to this study as particles simulated in slurry pipelines are highly similar to wells drilled with cuttings involved.

The experimental data to be simulated are as follows:

*Table 3:1. Experimental data sets to be modelled with hydrodynamic simulations.*

Source	Pipe Diameter	Particle Size	Solid Volume Concentration	Particle Specific Gravity	Mixture Velocity
Gillies et al [13]	103 mm	90 $\mu\text{m}$	10-45%	2.65	2.0-8.0 m/s

Once the model is confirmed to be valid, a drillpipe is added to the simulation. The eccentric annular geometry is represented by two cylinders positioned so that the inner cylinder moves with a uniform rpm, and the outer cylinder is stationary. The average fluid velocity in the eccentric annulus is computed relative to the moving inner pipe. During drilling, the pipe velocity can be assumed to be the rate of penetration. The following assumptions are applied the base setting:

- 1) steady-state, multi-phase, incompressible fluid flow;
- 2) the flow is isothermal with constant fluid properties;
- 3) slip effect is not considered;
- 4) closed end pipe, i.e, no communication between the inside of the inner pipe and the annulus.

### 3.2.2 Benchmark Problem by Founargiotakis

When it was determined that two phase simulations of solid particles and liquid would be too resource-intensive, a decision was made to conduct simulations with single phase flow of non-Newtonian Yield Power Law fluid. Therefore, a new benchmark problem was simulated. The effect of cuttings could still be simulated with the use of cutting volume fraction, with the following assumptions:

- 1) the cutting solids are finely mixed with the drilling fluid;
- 2) the mud rheology is altered accordingly due to the inclusion of cuttings;
- 3) laminar flow of drilling fluid, monitored by the calculated Reynold's Number.

The experimental data to be simulated are as follows:

*Table 3:2. Experimental data set from Okafor and Evers [24] to be modelled with simulations.*

Variable	Symbol	Unit	Value
Yield Stress	$\tau_0$	Pa	0.622
Consistency Index	$K$	Pa.s <sup>n</sup>	0.11934
Power Low Exponent	$n$	-	0.75534
Density	$\rho$	kg/m <sup>3</sup>	1066.2
Hole Size	$D_h$	mm	77.27
Drill Pipe Outer Diameter	$d_o$	mm	48.26
Mean Velocity	$m/s$	m/s	0.7-1.2

The length of the simulated section of the well is determined by the entrance length of a laminar flow in a pipe. An entrance region refers to a section of pipe up to when the velocity profile is fully developed.

In the case of laminar annular flow, the entrance length is  $3D_h$ . The resultant minimum length of section for fully developed flow is 0.232m, and 0.3m is taken for simplicity.

### 3.3 Solution Method and Performance Evaluation Parameters

This section discusses the solution method and the parameters that will be monitored as outputs for evaluation purposes.

#### 3.3.1 Simulating Benchmark Problem by Ekembara

To initialise the model validation, a geometry was reproduced with the selected data set from the experimental study conducted by Gillies [13]. The pipe simulated has a diameter of 103mm and a simulated length of 3m. A coarse mesh with maximum mesh size of 0.1m was initially used. Convergence was achieved at 85 iterations. Subsequently, refinement to the mesh is done until mesh independence is achieved with no changes to the simulation result with further refinement. The chosen mesh size required 640 iterations to converge. The resulting discretization of the geometry resulted in 322244 cells with the grid structure shown in Figure 3.2.

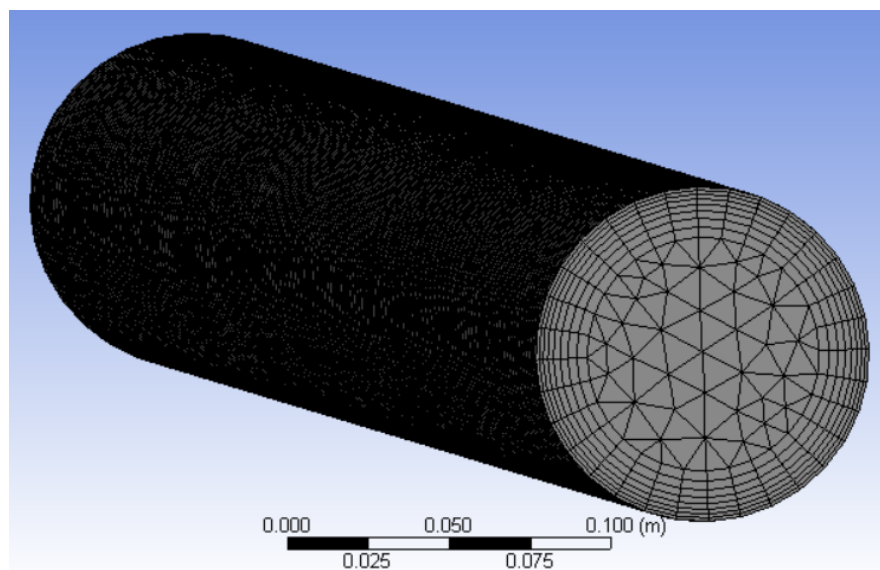


Figure 3:2. Grid structure for the benchmark validation simulation



The parameters of the simulation is summarized in the table below:

*Table 3:2. Summary of simulation parameters*

Boundary Condition	Inlet : Water at 3 m/s Outlet : Atmospheric pressure No-slip condition at wall
Particle Injection	Sphere with 90 micrometer particle size. Particle specific gravity of 2.65 Particle mass flow rate of 20 kg/s with 0 m/s initial velocity. Restitution coefficient of 0.9
Mathematical Modelling	Two-equation k-epsilon turbulence model was employed with the kinetic theory of granular flow. Drag forces were also taken into account for the simulation.
Numerical Solution	Three dimensional transient simulation with a constant time step of 0.05s The time averaged distribution of flow variables are computed over a period of 100s. The time step is adjusted to obtain a courant number of 20.41. This cuts down time needed to run the simulation.

The results from the study conducted by Ekambara [13] that are to be replicated are as shown in Figure 3.3.

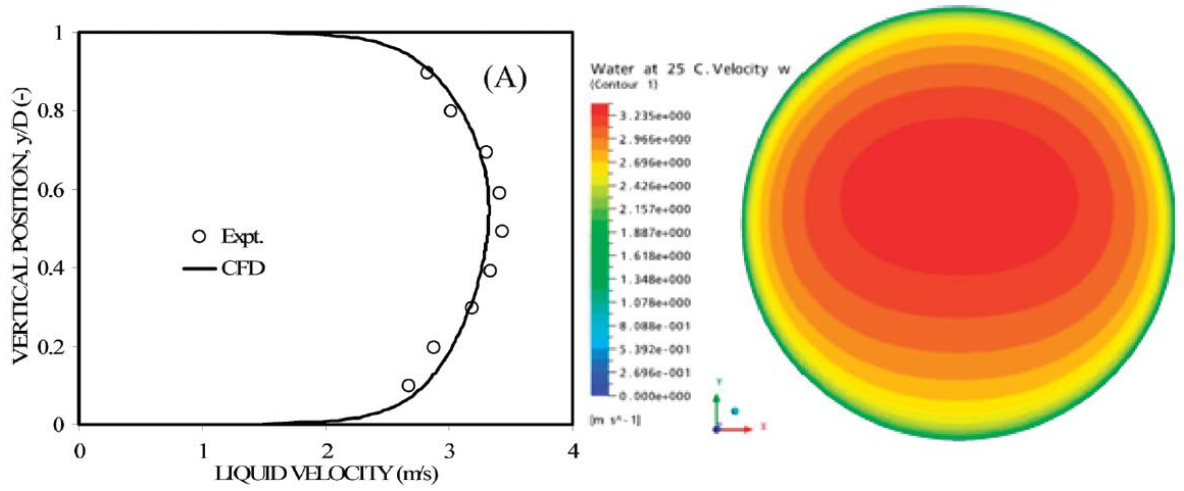


Figure 3.3. Predicted liquid velocities for the selected data set by Ekambara [13].

The validation simulation produced the result in Figure 3.4.

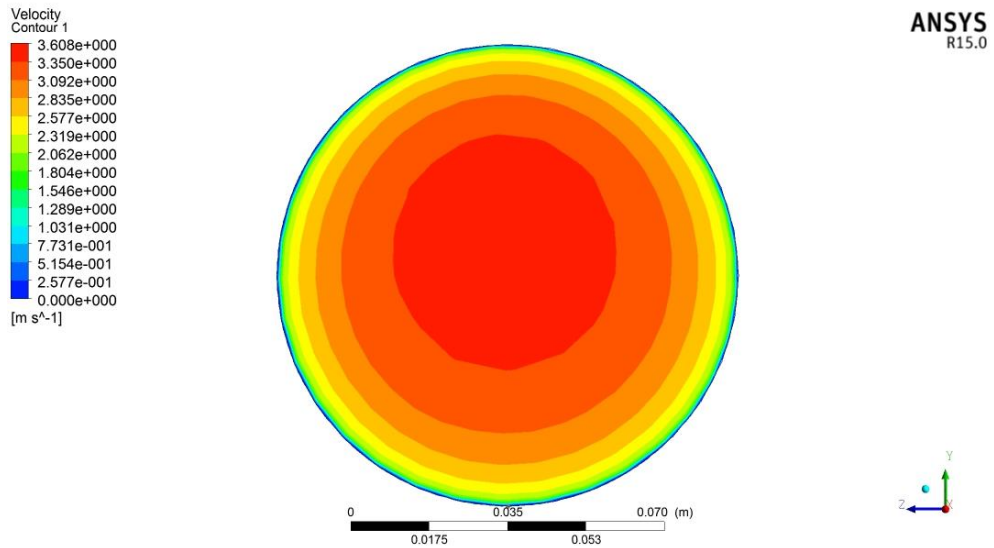


Figure 3.4. Velocity contour plot from the validation test simulation.

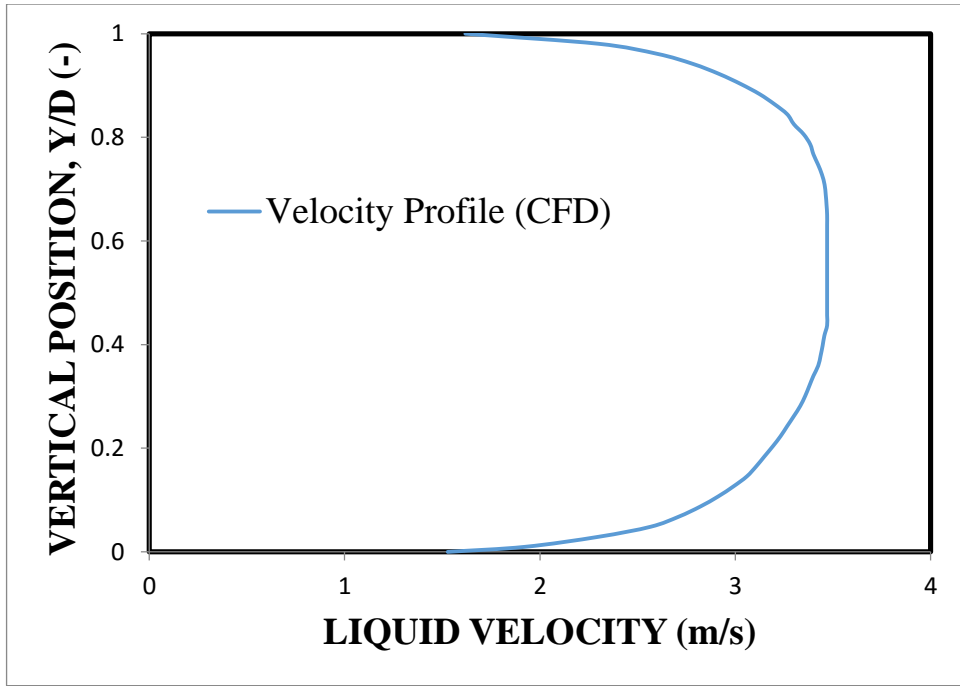


Figure 3:5. Liquid velocity profiles obtained from this project simulation.

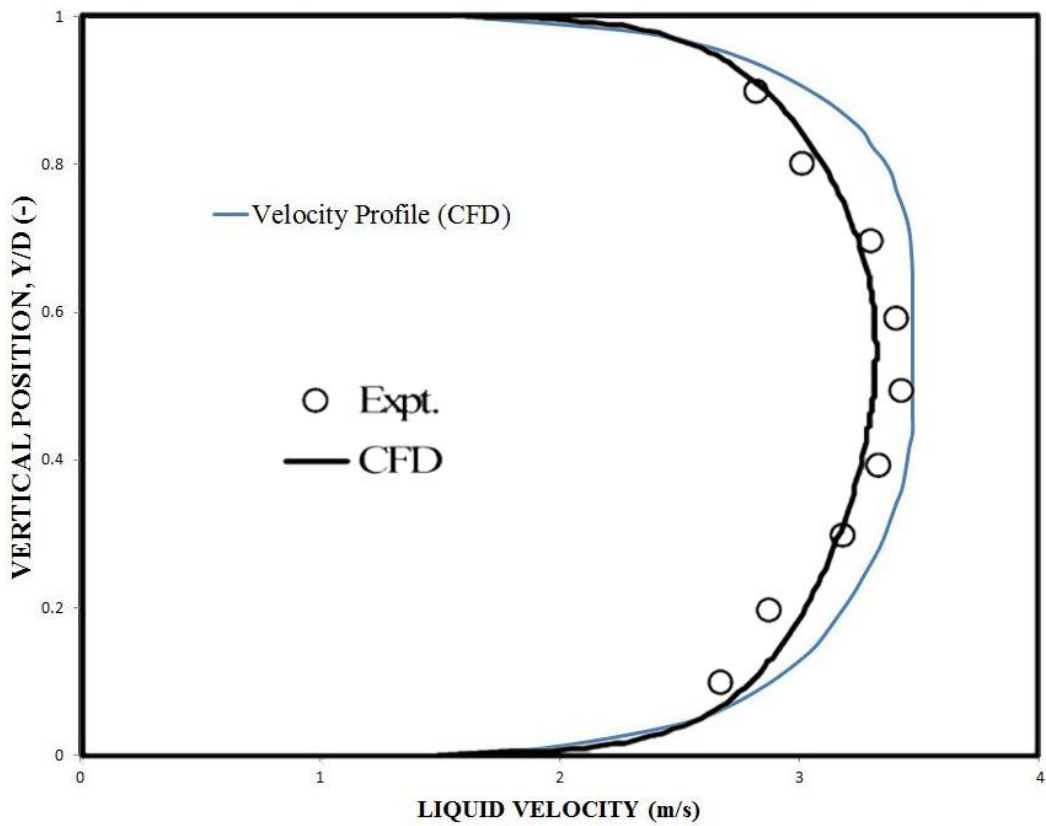


Figure 3:6. Comparison of the liquid velocity profiles obtained by Ekambara (2009) with the validation test result showing reasonable agreement.

Overall, the validation test results are in reasonable agreement with the simulations conducted by Ekambara. The sensitivity analysis showed that the simulation conducted by this project is a better match of the peak liquid velocity from the experimental study conducted by Gilles compared to Ekambara's study [13].

### 3.3.2 Simulating Benchmark Problem by Founargiotakis

The geometry was reproduced with the selected data set from the experimental study conducted by Okafor and Evers [24]. The geometry and meshing of the model was conducted. Refinement to the mesh was done until mesh independence is achieved with no changes to the simulation result with further refinement. Meshing with maximum mesh size of 0.078m was used. Convergence was achieved at an average of 20 iterations. The resulting discretization of the geometry resulted in 262600 cells with the grid structure shown in Figure 3.7.

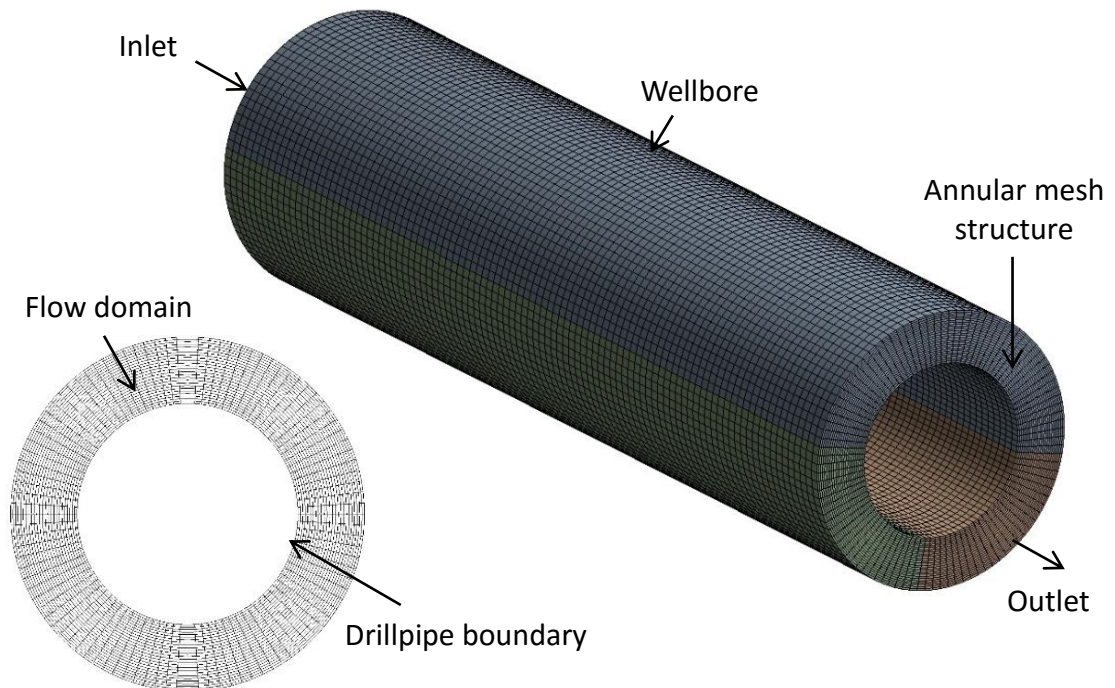


Figure 3:7. Simulated Well geometry

The parameters of the simulation is summarized in the table below:

Table 3:3. Parameters simulated from the data set from Founargiotakis's Study[15].

Boundary Condition	Inlet : Herschel-Bulkley fluid with properties provided by Okafor and Evers [24] at 0.7-1.2 m/s Outlet : Atmospheric pressure No-slip condition at wall
Mathematical Modelling	No turbulence model was used. Laminar condition is simulated
Numerical Solution	Steady State analysis
Convergence Criteria	RMS residual type with a target of 0.0001

The desired output is the change in pressure per unit length. This is obtained with the CFX expression language which allows custom outputs to be obtained. The screenshot below shows the simple coding, highlighted and named delPbydelL, used to obtain the results:

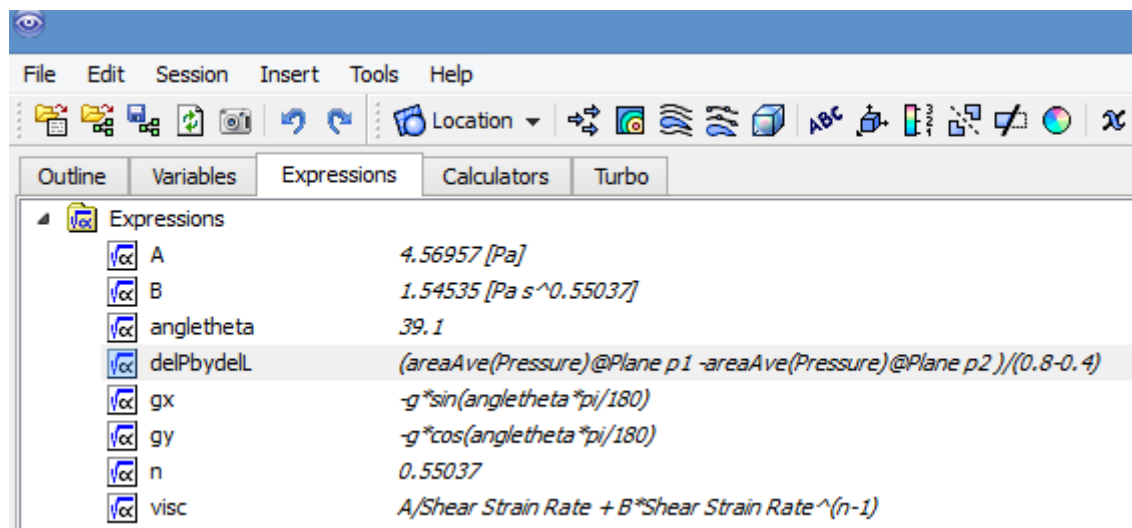


Figure 3:8. Screenshot of the CFX Expressions used to obtain the change in pressure over length

The benchmark simulations show the dependability of the model used. Comparisons of predictions from the approach in this work with the experimental results of Okafor and Evers, and the simulation work from Founargiotakis is shown in Table 3:4. While Founargiotakis’s work yielded excellent results, with an average deviation of 13.7%, the model used for this study managed an average deviation of only 7.8%. According to Founargiotakis [24], the cause for the large deviation in the last four points are unknown. The model used for this work showed better consistency at higher mean velocities, further solidifying the precision and accuracy of the model used for this work.

*Table 3:4. Comparison table of the results obtained by Founargiotakis and the simulation conducted for this study with the experimental results from Okafor and Evers [24].*

Experimental (Okafor and Evers, 1992)		Founargiotakis (2008)		Simulation	
Mean Velocity (m/s)	dp/dL (Pa/m)	dp/dL (Pa/m)	Deviation (%)	dp/dL (Pa/m)	Deviation (%)
0.440865	927.632	1026.32	9.615	1069.74	13.284
0.562019	1164.47	1203.95	3.279	1267.58	8.1343
1.01298	2092.11	1835.53	13.978	2208.4	5.2658
1.09375	2269.74	1934.21	17.3471	2407.08	5.705
1.12067	2309.21	1973.68	17.0	2472.44	6.601
1.22837	2526.32	2092.11	20.754	2739.97	7.797

From Figure 3:9, it is evident that the model used in this study has better consistency throughout the simulated mean velocities with the predictions from Founargiotakis becoming increasingly inaccurate at higher mean velocity.

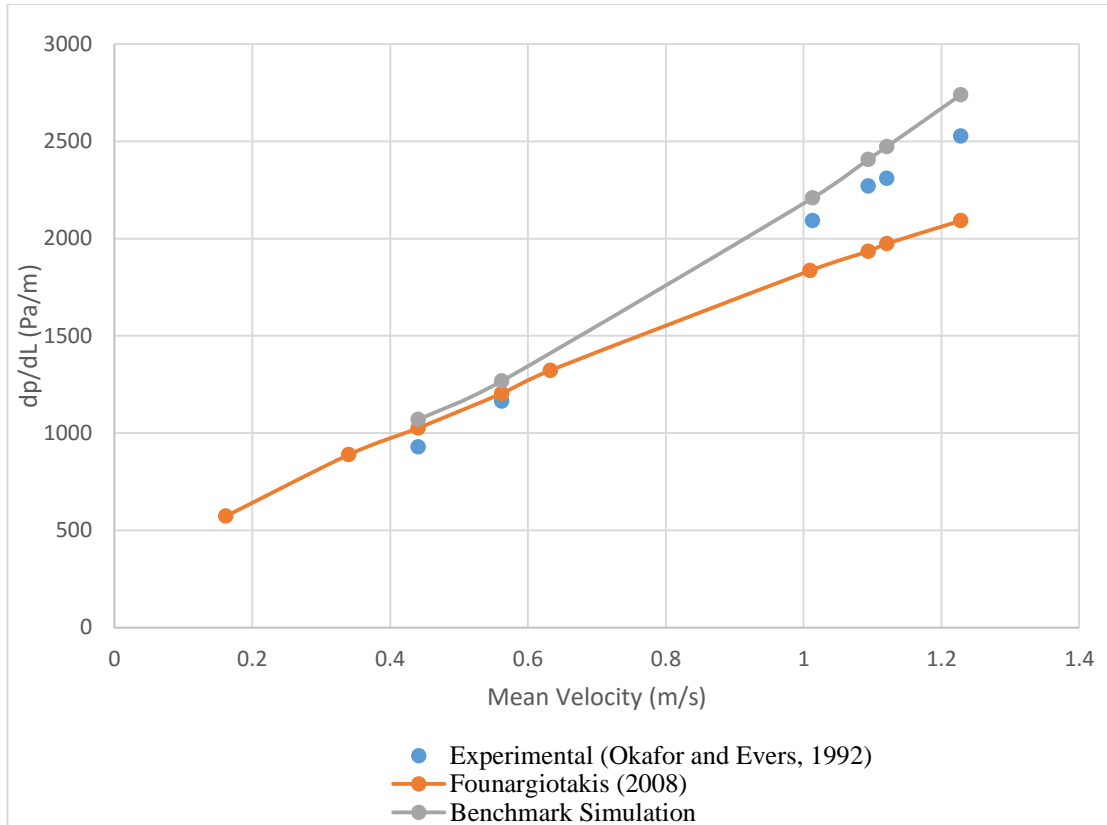


Figure 3:9. Comparison of predictions with data of Okafor and Evers(1992) with results obtained from the simulation by Founargiotakis (2008) [24].

### 3.4 Parametric Study and Regression Analysis

The effects of different drillpipe rotational speeds, cutting volume-fraction, eccentricity with Yield Power Law drilling fluid on cutting transport efficiency at the horizontal sections of a well. Regression analysis will be used to determine the relationship of the proposed drilling parameters on the . The assumptions made for the parametric study are:

- 1) steady-state, single-phase, incompressible fluid flow;
- 2) the flow is laminar and non-isothermal with changing fluid properties;
- 3) closed end pipe, i.e, no communication between the inside of the inner pipe and the annulus

### 3.4.1 Design of Experiment and Response Surface

Actual drilling parameters are analysed and the range of parameters are obtained from drilling reports. The design of experiment is with the varied conditions below:

Table 3:5. Simulation Parameters

Variable		Symbol	Unit	Drilling Stage		
				Min.	Max	Average
Volume Flow Rate		$q$	gpm	100	1000	450
Ratio of Hole dia to Pipe dia		$\kappa$	-	1.6	3.6	2.6
Volume Fraction of Cuttings		$\phi$	-	0	0.26	0.13
Drill Pipe Eccentricity		$\varepsilon$	-	0	0.85	0.425
Drill Pipe Rotation		$\Omega$	rpm	0	140	70
Drilling Direction		$\theta$	°	0	90	45
Mud Rheology	Yield Stress	$\tau_0$	Pa	0.175	11.84	6.0075
	Consistency Index	$K$	Pa.s <sup>n</sup>	0.031	8.431	4.231
	Power Law Exponent	$n$	-	0.229	0.82	0.5245

Table 3:6. Geometric data for annular flow simulations

Variable		Symbol	Unit	Drilling Stage		
				Surface	Intermediate	Production
Hole Size		$D_h$	in	17.5	12.25	8.5
Estimated Depth		$L_d$	ft	1500	7500	11500
Drill Pipe	Outer Diameter	$d_o$	in	5		
	Inside Diameter	$d_i$	in	4.276		



The key design parameters are determined from Table 3:5. The various combinations of parameters are set using the Parameter Set feature under Response Surface in ANSYS. The average initial parameters are used as inputs and a range of values for the parameters are generated in the Design of Experiment tab. Design of Experiment allows many variation of runs to be conducted with marginally more effort that is needed for a single run. A Design of Experiments is a scientific way to conduct a series of experiments with a given set of parameters, each with a range that minimizes the number of runs needed to understand the influence of the parameters [8]. The Custom + Sampling algorithm is used to import the results from an excel sheet. Subsequently, the results tabulated from the Response Surface tab, which allows efficient correlations to be analysed. There are five response surface types available, which are

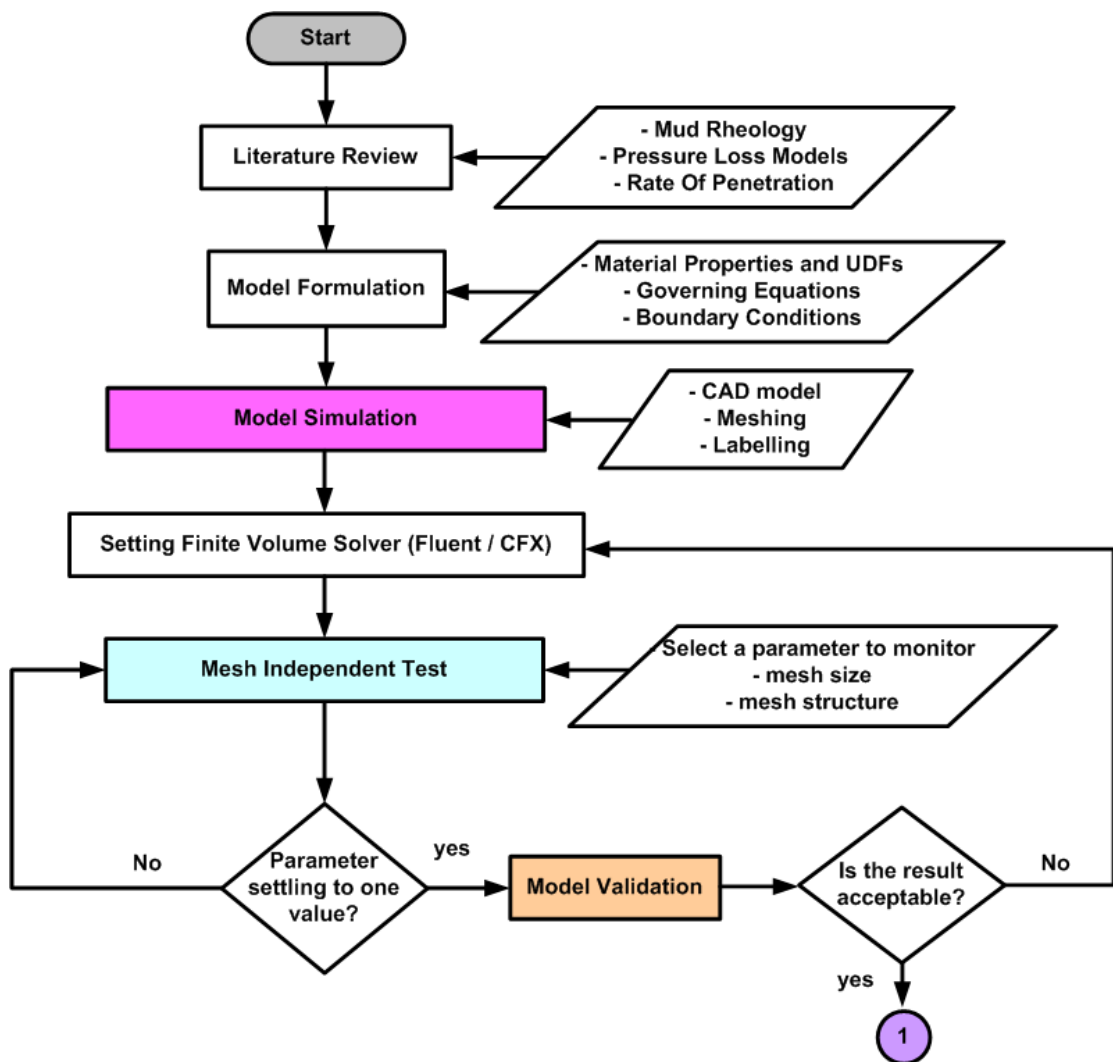
- 1) Standard Response Surface (2nd order polynomial) [the default]
- 2) Kriging
- 3) Non-parametric Regression
- 4) Neural Network
- 5) Sparse Grid

The response surface performance is determined by the Coefficient of Determination. It measures how well the response surface represents output parameter variability. The best performing response surface for the data given should have a value as close to 1.0 as possible. Another method is to monitor the Adjusted Coefficient of Determination, which takes the sample size into consideration when computing the Coefficient of Determination. This is more reliable than the usual coefficient of determination when the number of samples is small ( $< 30$ ). Lastly, the Maximum Relative Residual can be monitored. It is a similar measure for response surface using alternate mathematical representation and should be as close to 0.0 as possible.

The approach is not without its flaws however. This approach is a trial and error approach requires some time in order to get an appropriate parameter set for the goal to be achieved. To get reliable information, the number of configurations to examine can be quite important if the number of input parameters is high. In this case 10 parameters are investigated, which is still manageable by the software.

### 3.5 Summary

The methodology for this study can be simplified into the flow chart in Figure 3:10. A literature review was conducted to determine the areas to be studied. A model is then created based on relevant prior studies. Once the model is validated, work is done on the parametric study to obtain the correlation between the desired parameters and the pressure gradient in the annulus. Analysis is conducted from the response surface results.



(a)

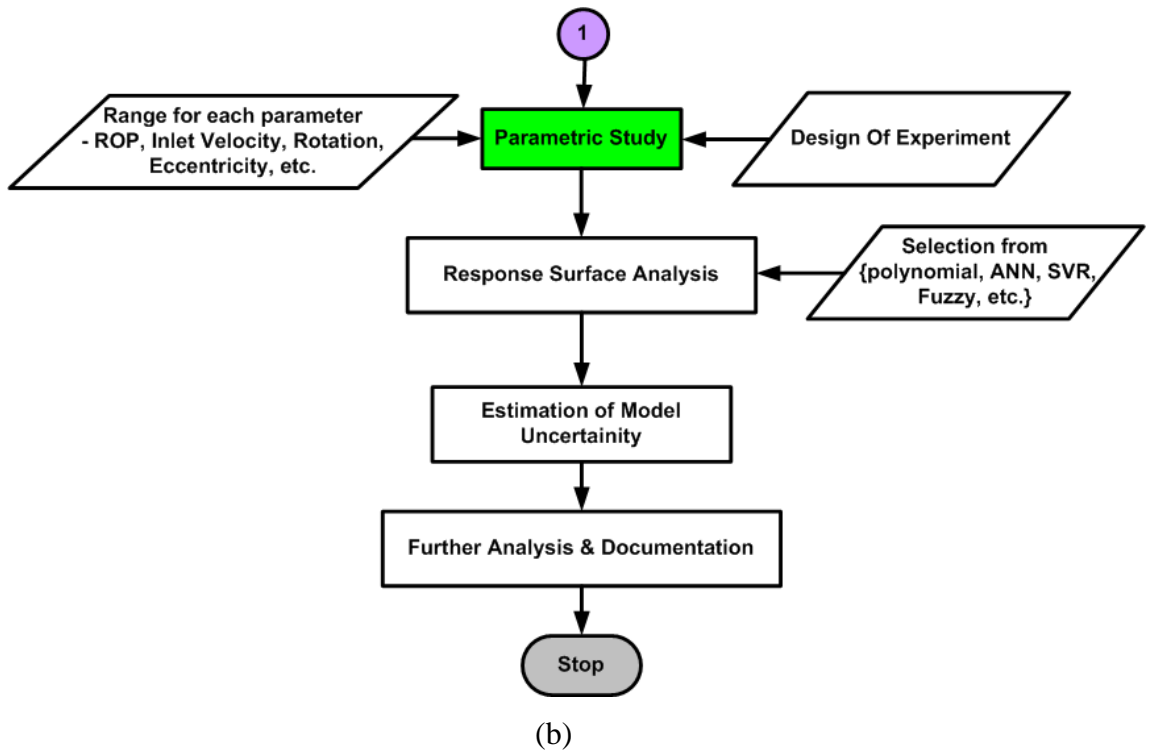


Figure 3:10. Project Flow Chart

## **CHAPTER 4 : RESULTS AND DISCUSSION**

### **4.1 Introduction**

Annular flow in managed pressure drilling has been the center of numerous studies since the importance of drilling fluids was realized. However, the effects of drilling parameters on the pressure gradient have only yielded simple implicit correlations. This study will address the effect of cuttings, mud flow rate, inclination, drill pipe rotation, and mud rheology on the pressure gradient in annulus. The key strength of this study is that the effect of each parameter can be analyzed relative to one another.

#### **4.1.1 Model and Simulation Setting**

The model used for the parametric study is based on the foundations laid by the benchmark study. In this case, the model generated for the benchmark study of Founargiotakis's work will be used as a base. Accurate and precise results were obtained from the benchmark study, which serves as a good basis for the simulations in this study. The parameters and simulation settings are described in the methodology section of this work.

### **4.2 Simulation**

Three main simulations were conducted. The first investigates the effect of cuttings on the pressure gradient in annulus with the use of 0.26 cutting volume-fraction, given the same drilling fluid rheology. The second investigates the impact of cuttings, mud flow rate, inclination, drill pipe rotation, and mud rheology on the pressure gradient in annulus. The third determines the relationship between Reynolds, Froude, Taylor and Bingham dimensionless numbers and the pressure drop for flow in annulus.

#### 4.2.1 Case-1: Model Verification and Effect of Cutting as a Density and Viscosity Modifier on the Pressure Gradient in Annulus

According to Figure 4:1, there is an excellent agreement between the simulation results and the experimental data (average deviation of 8%) for pressure drop of a unit length with different flow rates. The model was validated with the observation that the simulation results are able to predict experimental data under a range of flow rates.

The introduction of cuttings as a volume-fraction has a profound effect on the pressure drop through annulus. The assumption is made that the cuttings are finely mixed with the drilling fluid, without cutting bed formation. This enables single phase simulations to be conducted, with the viscosity and density of the drilling fluid appropriately modified with equation 3.5 and 3.6. Figure 4:1 shows the large difference in pressure drop between the simulations with and without cuttings volume-fraction. The simulation with cuttings is on average 56% higher than the simulations without cuttings, and shows a minor but steady decrease in percentage difference at higher flow rates.

*Table 4:1. Pressure drop results by simulation with and without 0.26 cutting volume-fraction with the percentage of difference.*

Experimental (Okafor and Evers, 1992)		Simulation	Simulation With Cutting (0.26 vol fraction)	
Mean Velocity (m/s)	dp/dL (Pa/m)	dp/dL (Pa/m)	dp/dL (Pa/m)	Difference (%) vs no cutting
0.440865	927.632	1069.74	2666.81	59.88690608
0.562019	1164.47	1267.58	3153.14	59.79943802
1.01298	2092.11	2208.4	4926.13	55.16967681
1.09375	2269.74	2407.08	5277.96	54.39374304
1.12067	2309.21	2472.44	5397.42	54.19218812
1.22837	2526.32	2739.97	5892.19	53.49827483

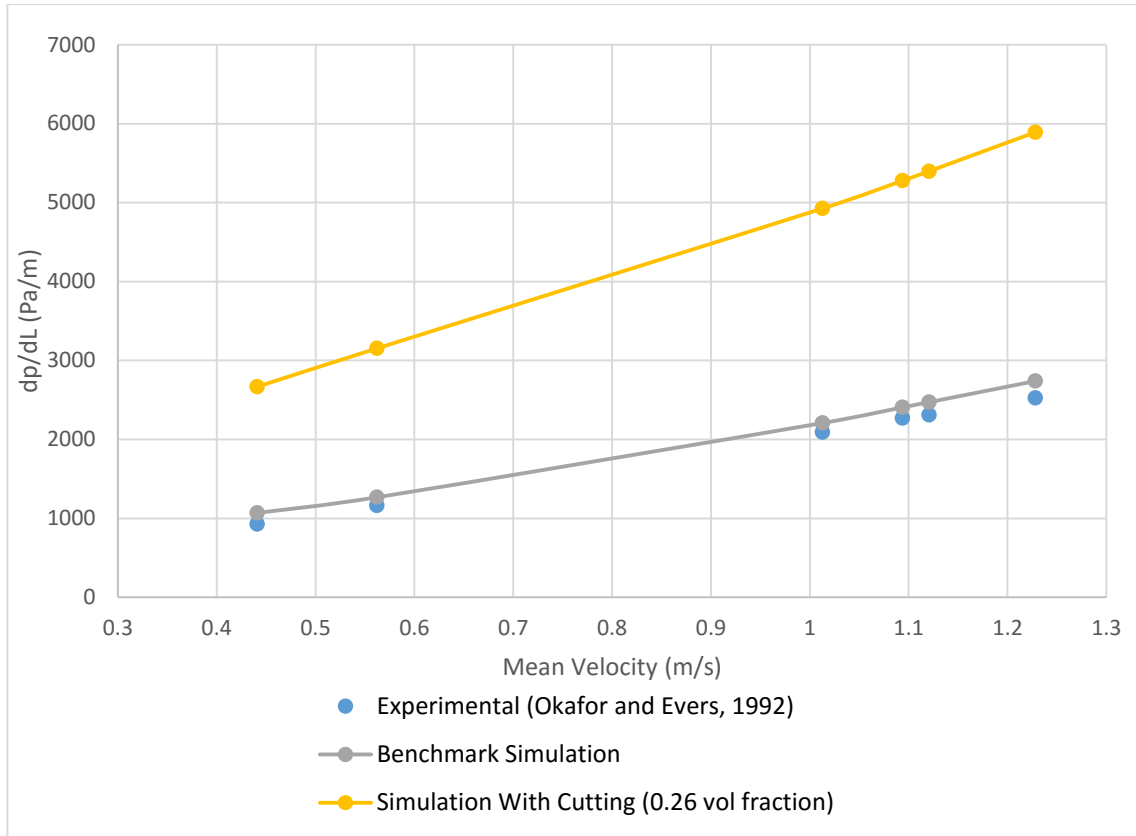


Figure 4:1. Comparison of simulations with and without 0.26 cutting volume-fraction

#### 4.2.2 Case-2: Effect of cutting volume-fraction, mud flow rate, inclination, drill pipe rotation, and mud rheology on the pressure drop in annulus

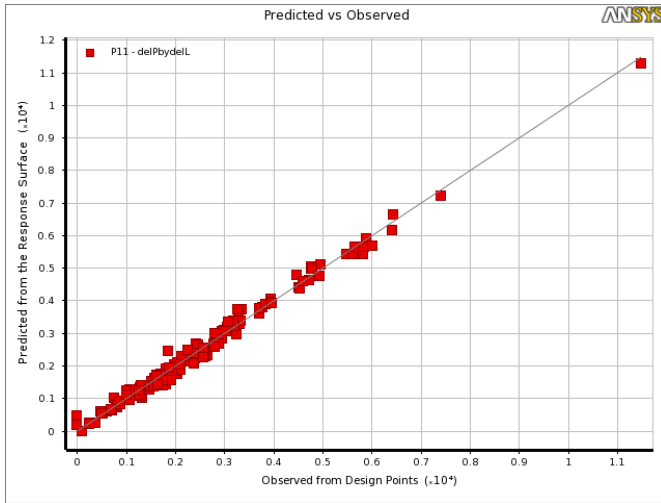
A total of 294 simulation runs were carried out in two Design of Experiment (DOE) algorithms, namely Central Composite Design and Latin Hypercube sampling technique. The influence of cutting volume-fraction, mud flow rate, drill pipe rotation, inclination, and mud rheology on pressure drop through the annulus can be determined with the minimal amount of runs with the DOE. Once the simulation is completed and the result of the two sampling technique is obtained, the data is combined and exported into an excel sheet where irrelevant or illogical results are filtered out. The usable data after filtering the collective results is 139 runs. The amount of data available is more than sufficient to draw a correlation between the input parameters and the pressure gradient. The resultant excel sheet is then re-imported into a new ANSYS Response Surface workbench where a response surface

analysis is conducted. Three response surface methods are used to tabulate the results, namely Standard Response Surface (2nd order polynomial), and Neural Network. The performance of these response surface methods for this study's application is compiled into Table 4:2 below.

*Table 4:2.. Performance result of the response surface types for drilling parameters study*

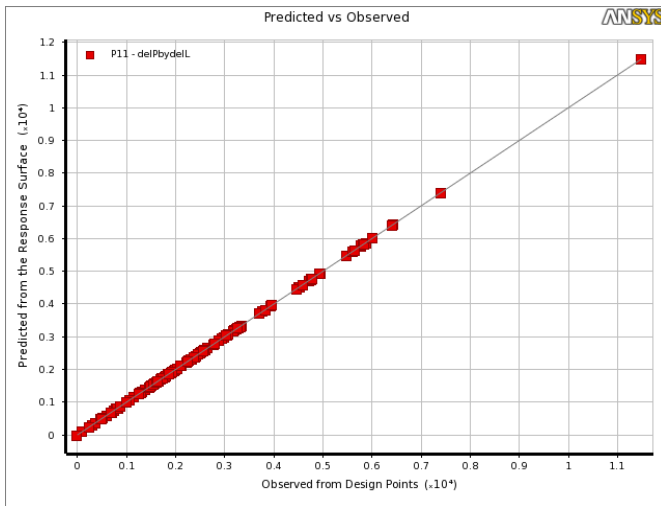
Performance Monitor	Full 2 <sup>nd</sup> order	Kringing	Neural Network
Coefficient of Determination (Best Value = 1)	0.98882	1	0.9867
Adjusted Coeff of Determination (Best Value = 1)	0.98624	-	-
Maximum Relative Residual (Best Value = 0%)	150883	0.0203	170133
Root Mean Square Error (Best Value = 0)	184.45	3.90E-05	201
Relative Root Mean Square Error (Best Value = 0%)	13341	0	14484
Relative Maximum Absolute Error (Best Value = 0%)	34.894	0	46.31
Relative Average Absolute Error (Best Value = 0%)	8.3276	0	8.9343

It is clear that Kringing is the best performing response surface and the results from this method will carry more weight during further analysis. Comparisons of Figure 4:2, Figure 4:3, and Figure 4:4 also show that Kringing response surface has the least variability in data predictions.



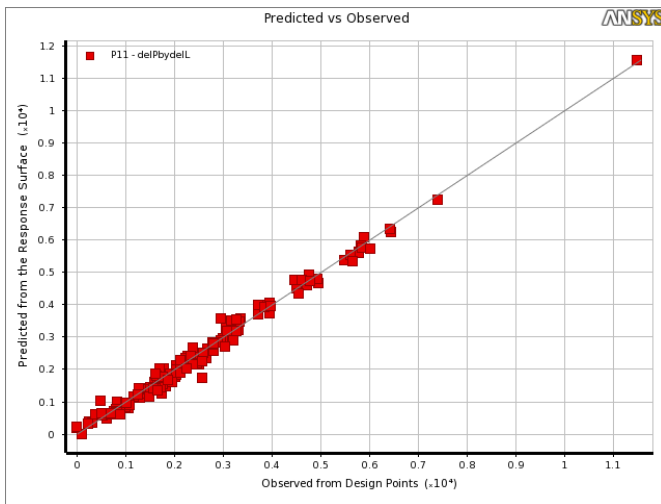
2<sup>nd</sup> Order Polynomial  
RMS Error = 13341

Figure 4:2. Goodness-of-fit graph for 2nd order polynomial response surface



Kriging  
RMS Error = 3.90E-05

Figure 4:3 Goodness-of-fit graph for Kriging response surface



Kriging  
RMS Error = 201

Figure 4:4. Goodness-of-fit graph for Neural Network response surface



The effect of each input parameter can be determined with Local Sensitivity. The result obtained from all three response surface types show a similar trend in input parameters of cutting volume-fraction ( $\phi$ ), inlet fluid velocity ( $v_{in}$ ), yield stress ( $\tau_0$ ), consistency index ( $c_0$ ), and Power-Law index ( $n$ ). A drastic difference can be seen for the drill pipe rotation ( $\omega$ ) where the 2<sup>nd</sup> order polynomial indicated higher pressure losses for the introduction of pipe rotation. The results from Kriging and Neural Network both indicated lower pressure losses with the introduction of drill pipe rotation.

Eccentricity ( $e$ ) is another parameter result that is conflicting. 2<sup>nd</sup> order polynomial method result indicates that eccentricity does not play a meaningful role in annular pressure gradient. Kriging however indicates that eccentricity plays a small role in causing annular pressure drop. Results from Neural Network on the other hand contradict this and indicates that eccentricity reduced the pressure drop in the annulus. Inclination ( $\theta$ ) yielded similarly contradicting results, where inclination results from 2<sup>nd</sup> order polynomial once again infers almost no effect on pressure gradient. Kriging method shows that inclination has contributions to the pressure drop in annulus and Neural Network indicating the opposite, where inclination helps reduce pressure losses in annulus.

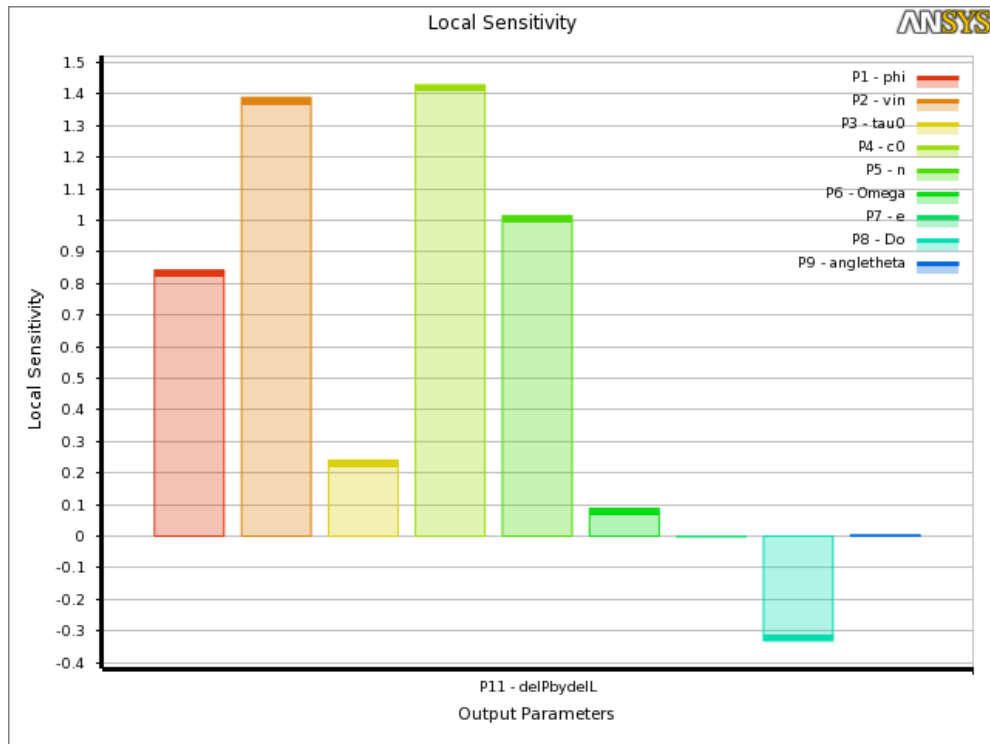


Figure 4.5. 2nd Order Polynomial Input Parameter Sensitivity

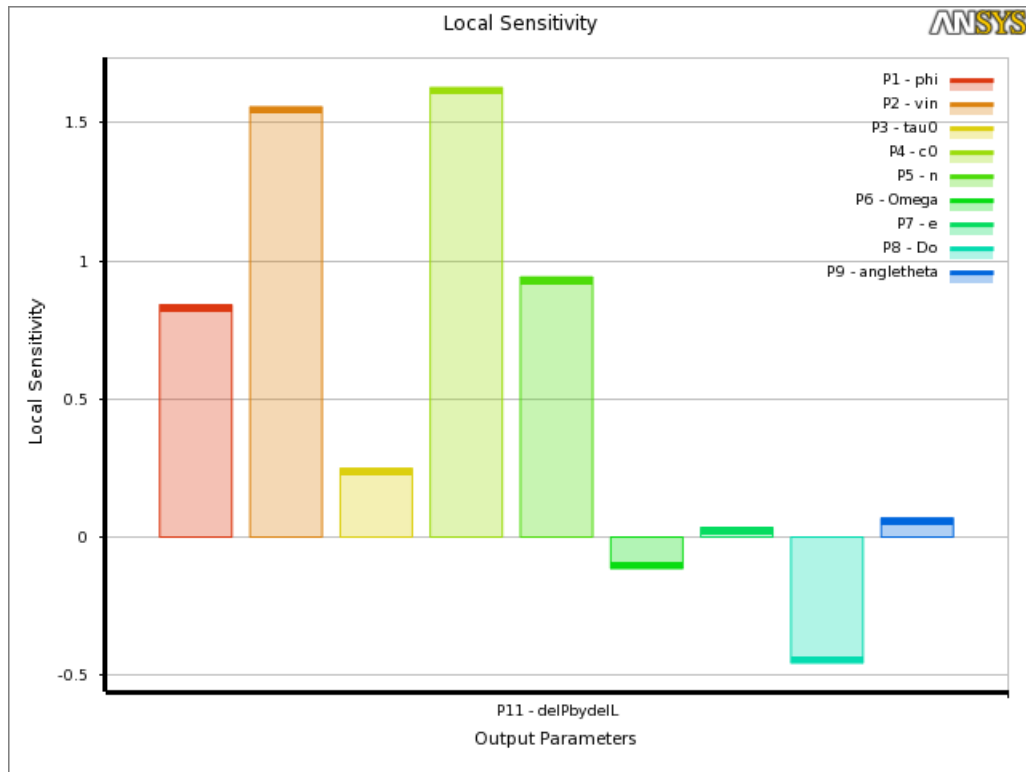


Figure 4.6. Kringing response surface Input Parameter Sensitivity

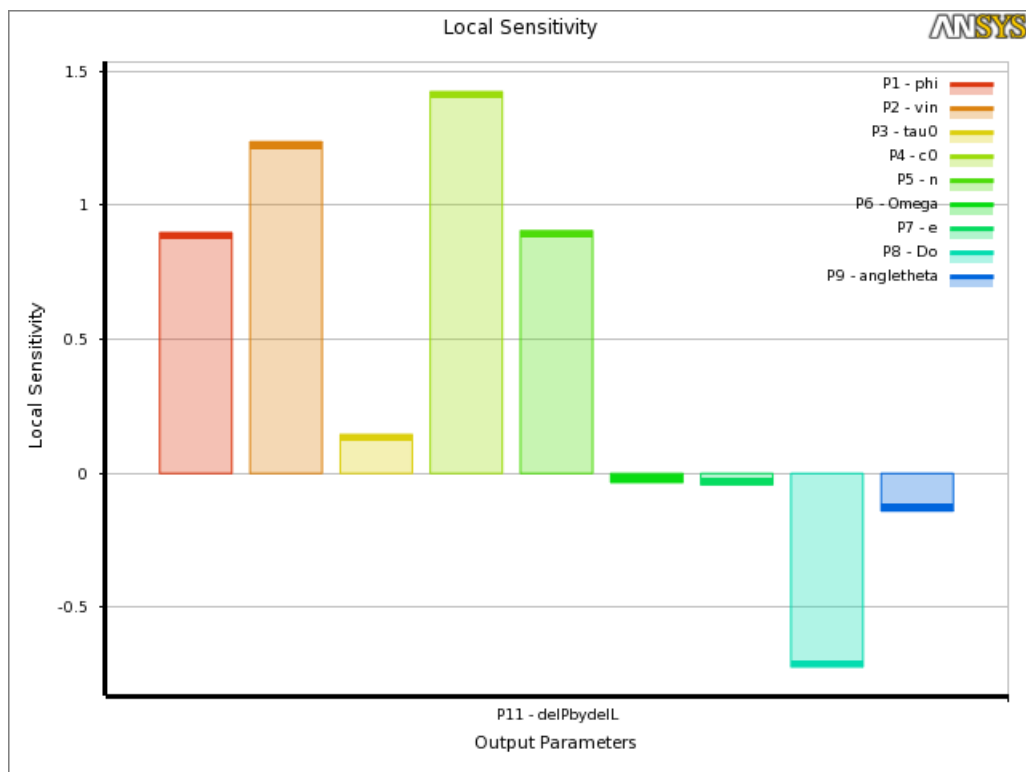


Figure 4.7. Neural Network response surface Input Parameter Sensitivity

### 4.2.3 Relationship between Reynolds, Froude, Taylor and Bingham dimensionless numbers and the pressure drop for flow in annulus

In GhasemiKafrudi's work [14], he developed a friction factor correlation where pressure drop was obtained from numerical simulations and the friction factor was tabulated with the Darcy-Weisbach equation. The friction factor correlation can be expressed as:

$$C_f = f_1(Bi, \varphi, Fr) \left(\frac{Bi}{Re}\right)^{f_2(n)} + f_3(Ta) \quad (4.1)$$

where

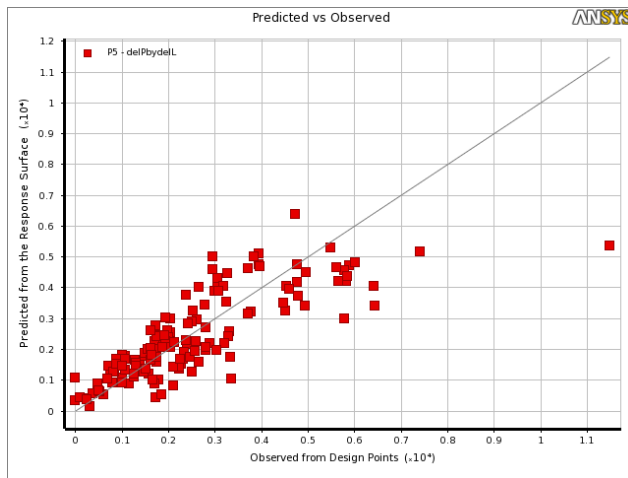
$$\begin{aligned} f_1(Bi, \varphi, Fr) &= 1.424(Bi.Fr^n)^{-0.666} + 2.845(\varphi)^{0.8998} - 0.3318, \\ f_2(n) &= -0.514n^{0.7899} + 1.015, \\ f_3(Ta) &= 0.0018Ta^{0.1285} \end{aligned}$$

Therefore, the prediction of pressure loss in annulus is a function of Reynolds, Froude, Taylor and Bingham dimensionless number. These dimensionless numbers are analysed further in this study due to its significance in characterising pressure drop in annulus. The dimensionless numbers are first manually calculated for each 139 runs with the use of an excel sheet. Similar to the study of drilling parameters, the resultant excel sheet is then re-imported into a new ANSYS Response Surface workbench where a response surface analysis is conducted. Three response surface methods are used to tabulate the results, namely Standard Response Surface (2nd order polynomial), and Neural Network. The performance of these response surface methods for this study's application is compiled into Table 4:3.

Table 4:3. Performance result of the response surface types for dimensionless number study

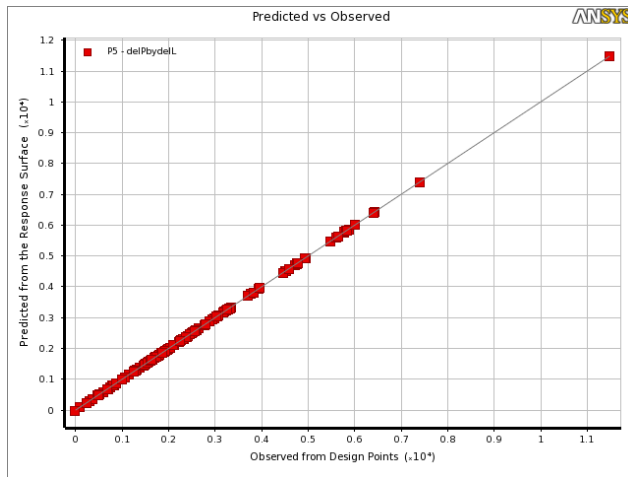
Performance Monitor	Full 2 <sup>nd</sup> order	Kriging	Neural Network
Coefficient of Determination (Best Value = 1)	0.6455	1	0.6667
Adjusted Coeff of Determination (Best Value = 1)	0.6295	-	-
Maximum Relative Residual (Best Value = 0%)	750295	0.11857	795102
Root Mean Square Error (Best Value = 0)	1038.6	0.000714	1007
Relative Root Mean Square Error (Best Value = 0%)	63472	0	67608
Relative Maximum Absolute Error (Best Value = 0%)	347	0	337.17
Relative Average Absolute Error (Best Value = 0%)	43	0	41.707

A similar trend can be seen in Table 4:3 as compared to the study of drilling parameters in Table 4:2. It is clear that Kriging is the best performing response surface and the results from this method will carry more weight during further analysis. Comparisons of Figure 4:2, Figure 4:3, and Figure 4:4 also show that Kriging response surface has the least variability in data predictions.



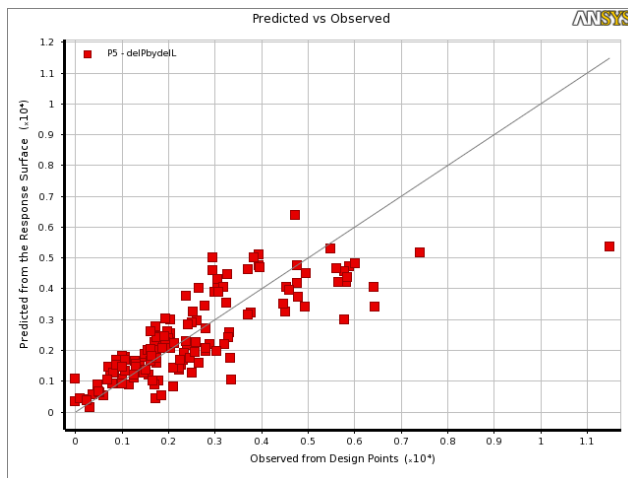
2<sup>nd</sup> Order Polynomial  
RMS Error = 1038.6

Figure 4:8. Goodness-of-fit graph for 2nd order polynomial response surface



Kriging  
RMS Error = 0.000714

Figure 4:9. Goodness-of-fit graph for kriging response surface



Neural Network  
RMS Error = 41.707

Figure 4:10. Goodness-of-fit graph for Neural Network response surface

The result obtained from all three response surface types show a similar trend for Reynolds (Re), and Froude dimensionless numbers, although the 2<sup>nd</sup> order polynomials obtained a difference in local sensitivity of 1 on average compared to the other two response surface types. For Taylor, Kringing and Neural Network results indicate that a higher number results in less pressure drop through annulus. 2<sup>nd</sup> order polynomials determined Taylor has no effects on pressure drop, while all three response surface linked Bingham number to the increase in pressure through annulus. The results from 2<sup>nd</sup> order polynomials are disregarded due to its poor performance in Root Mean Square error.

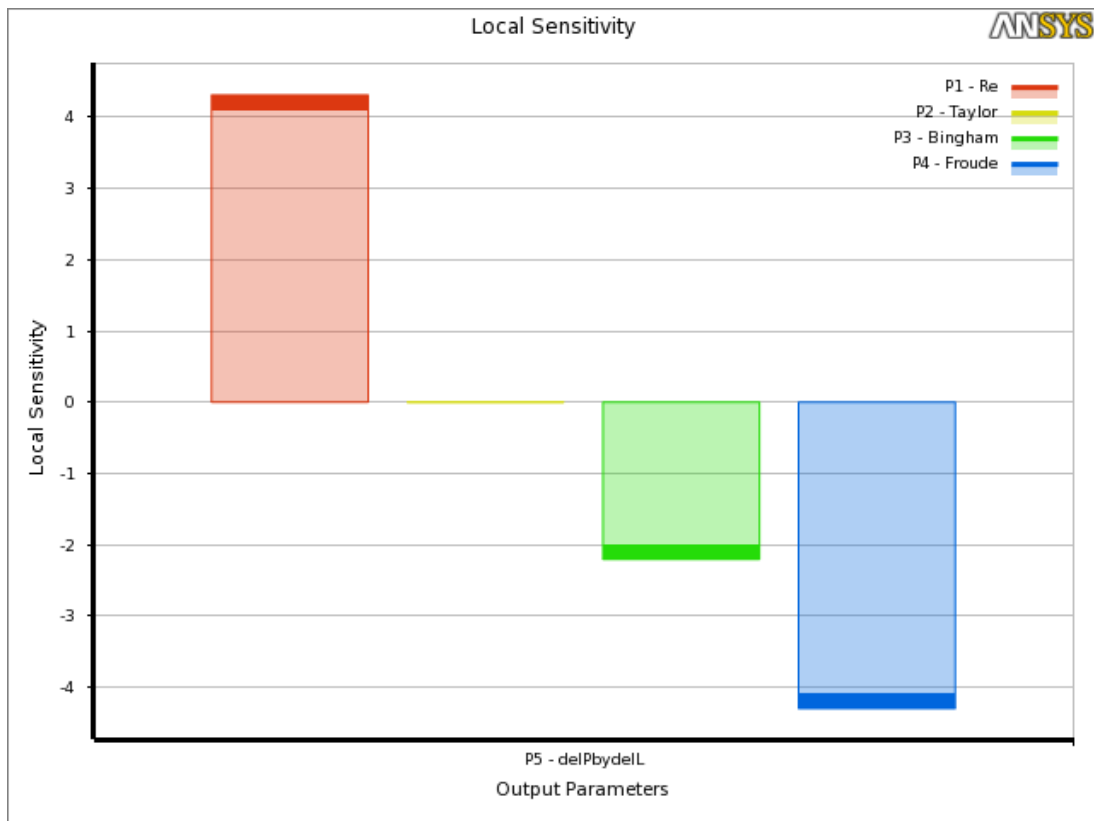


Figure 4:11. 2nd Order Polynomial Input Parameter Sensitivity

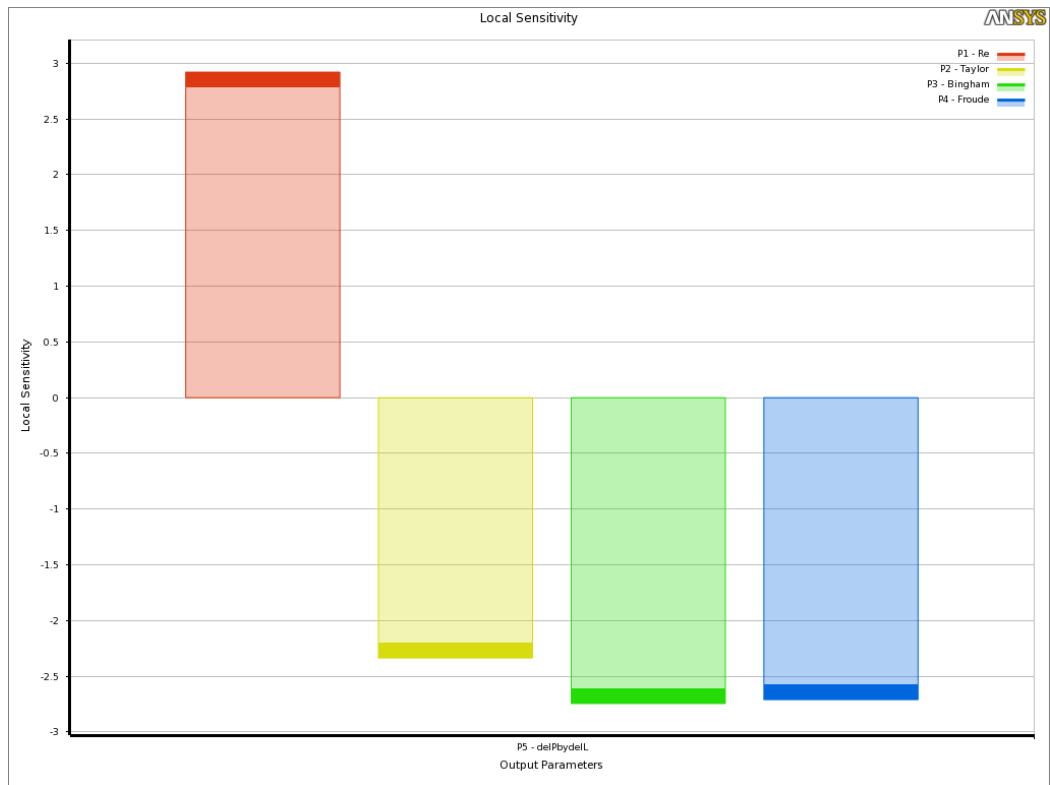


Figure 4:12. Kringing Input Parameter Sensitivity

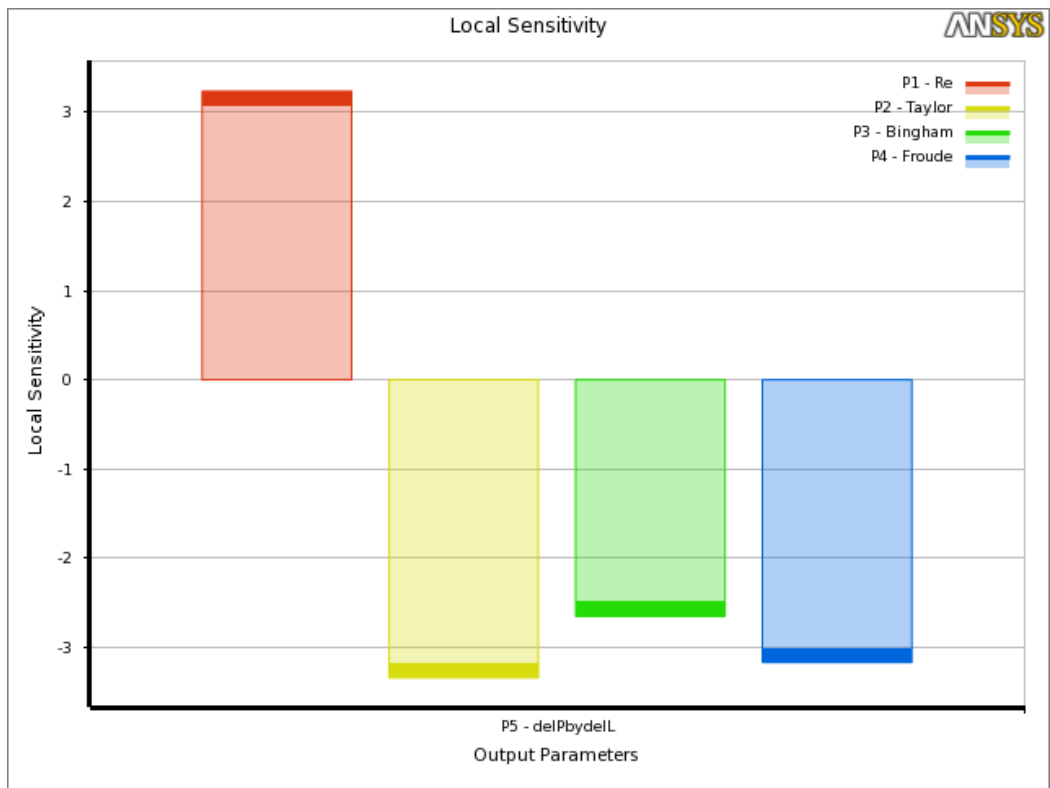


Figure 4:13. Neural Network Input Parameter Sensitivity

### 4.3 Discussion

This section discusses the results and inference obtained from the simulations conducted. Point of interest in this study is the effect of mud rheology, cuttings, and various drilling parameters on pressure drop in annulus.

#### 4.3.1 Influence of mud rheology on pressure drop

Results from Figure 4:6 indicate that the parameters within the Herschel-Bulkley fluid model which has a meaningful impact on pressure drop is the consistency index ( $c_0$ ), and Power-Law index ( $n$ ). The Shear Stress has a less significant impact because when the drilling fluid is already flowing, the yield stress has already been overcome. Yield stress will be more significant in studies of pipeline restart pressures for example but for study of flowing fluids, it can be not as critical. An inference can also be made that pressure gradient depends more on rheological parameters of drilling mud and fluid flow, and less on the drilling parameters. The result is in agreement with GhasemiKafrudi's work [14]. The 3D response chart in Figure 4:14 show that the combination of a high for the effect of consistency index ( $c_0$ ), and Power-Law index ( $n$ ) would lead to significant pressure drop.

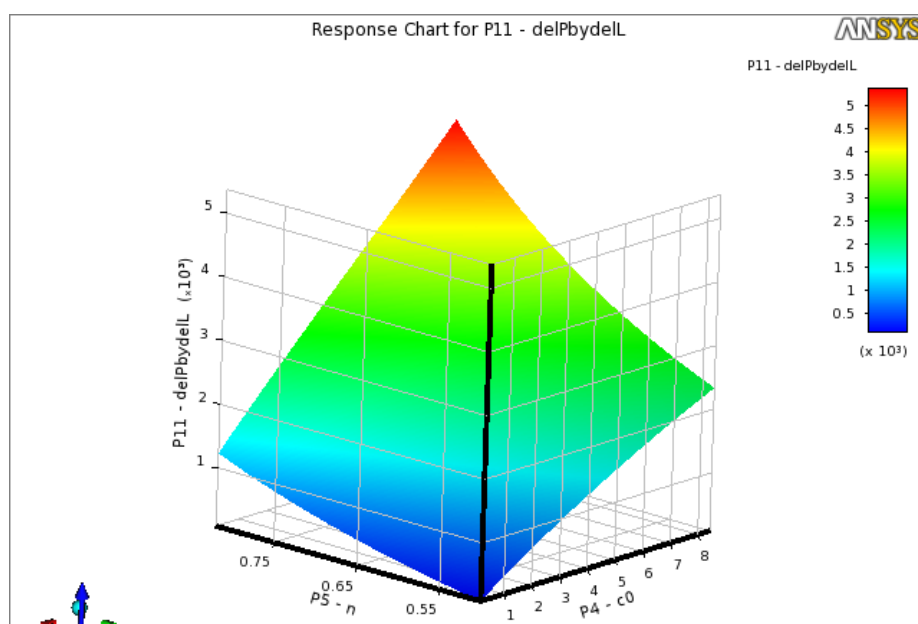


Figure 4:14. 3D response chart of consistency index, Power-Law index and Pressure Gradient



### 4.3.2 Effect of cutting volume-fraction on pressure drop

The effect of high cutting-volume fractions (0%-26%) were considered for this study. The effect of cutting volume-fraction has been well documented and is supported by this study. From the response chart of Figure 4.15, with a fluid velocity of 0.665 m/s, a significant increase in pressure drop of 1826 pa/m can be expected from just 0.1 volume-fraction of cuttings in the annulus. In on-the-limit drilling conditions, where up to 0.26 volume-fraction of cuttings can be expected, the pressure loss is in excess of 3400 pa/m. It should be noted that this study does not take into account the solid-fluid interaction which can increase the pressure drop. At higher cutting concentrations, bed formation can occur and the hydraulic pressure drop of fluid flow increases due to higher friction between the wall and mixture.

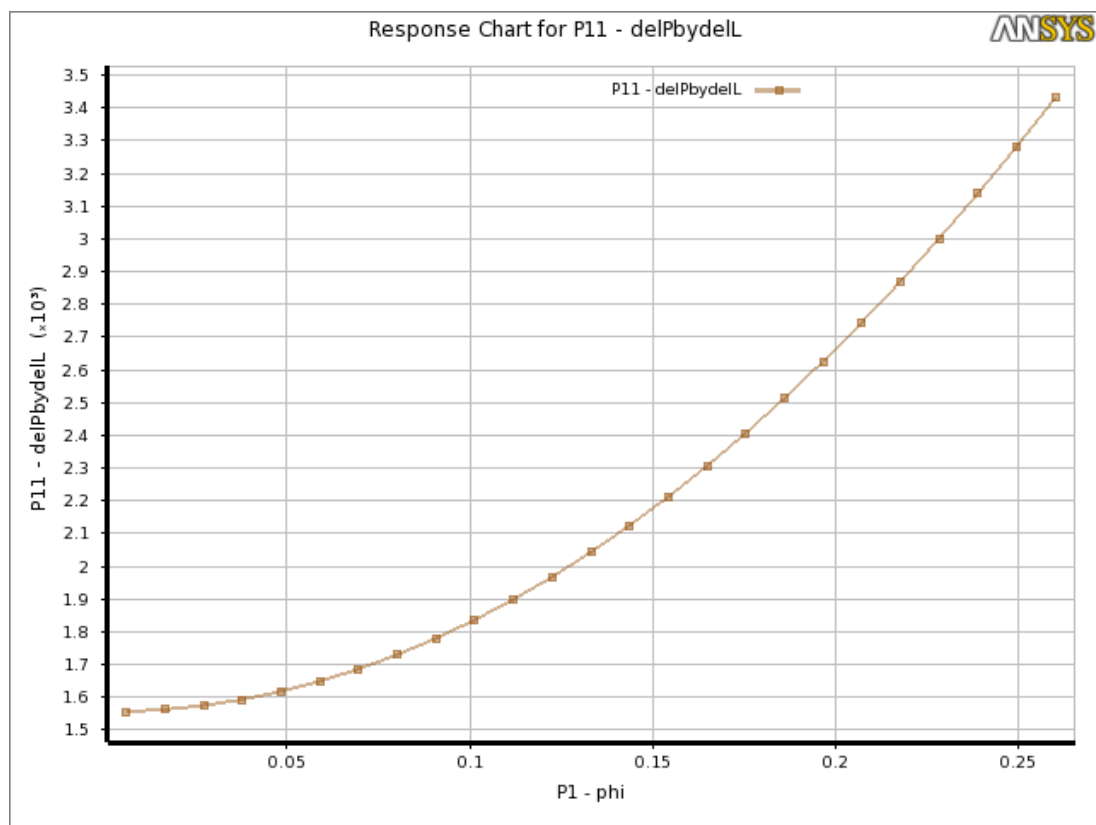


Figure 4:15. 2D response chart of pressure gradient and cutting volume-fraction ( $\phi$ ) at 0.665m/s fluid inlet velocity. Fluid properties are: Yield Stress = 5.9 Pa, consistency index = 4.3 Pa.s<sup>n</sup>, Power-Law index = 0.66.

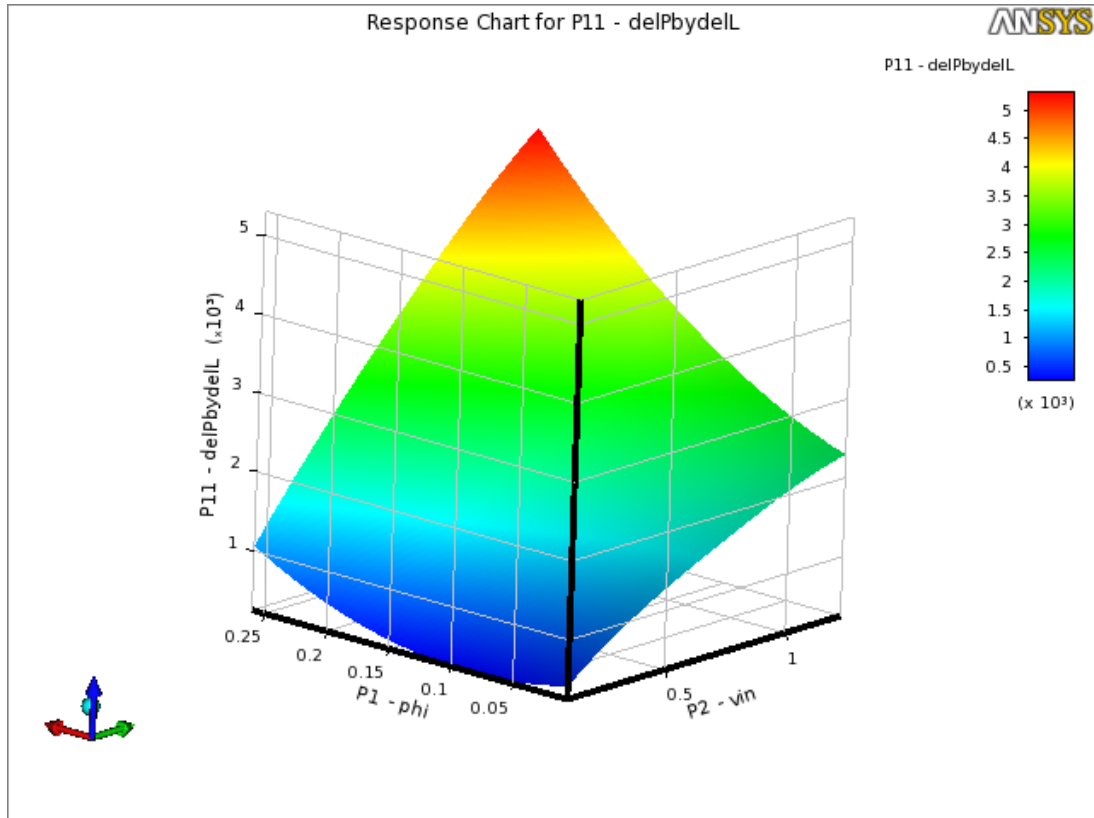


Figure 4:16. 3D response chart for cutting concentration( $\phi$ ), and fluid inlet velocity( $v_{in}$ ). Fluid properties are the same as Figure 4:15.

### 4.3.3 Influence of drilling parameters on pressure drop

The inference that can be made based on Figure 4:6 is the effect of eccentricity of drill pipe is negligible. The result is not necessarily bad as very little can be done in real drilling conditions with eccentricity. However, eccentricity in horizontal wells will cause cutting to settle at the bottom of the wellbore, potentially forming a bed. Critically, these cutting beds lead to an decrease of pressure in annulus [25].

Drill pipe rotational velocity has a small influence on annular pressure loss, according to Figure 4:6. Further investigation of the response chart for drill pipe rotational velocity and show that pressure loss reduction occurs with rotation until a threshold of 3.8 rad/s. From that rotational velocity onwards, the pressure drop reduces. This can be explained by the shear rate in Herschel-Bulkley fluids

increasing due to drill string rotation. Consequently, the drilling fluid viscosity decreases which leads to the results obtained by simulation.

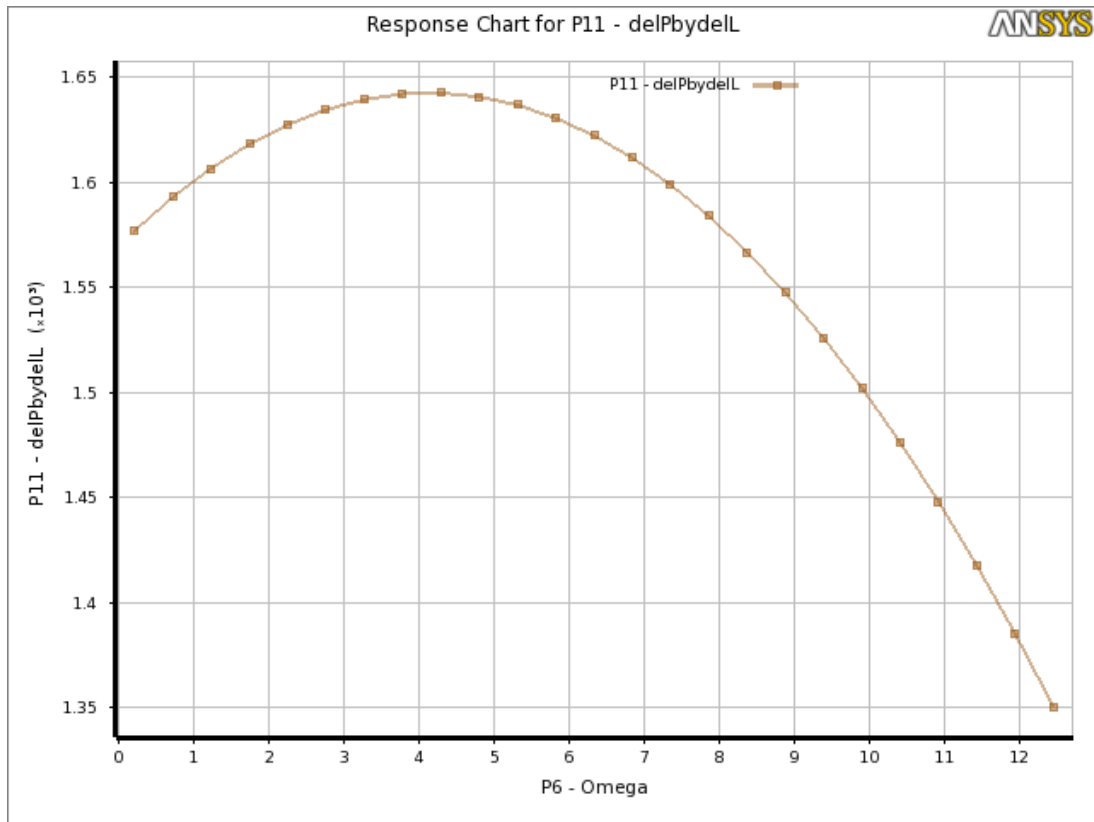


Figure 4:17. 2D response chart of pressure gradient against drill pipe rotational velocity ( $\omega$ ). Fluid properties are identical to fluid used in Figure 4:15.

## CHAPTER 5 : CONCLUSION AND RECOMMENDATION

### 5.1 Conclusion

This project has provided a literature review related to the effects of drillpipe rotation, cuttings, inclination, eccentricity and mud rheology on pressure drop predictions in annulus by modeling. A validation test was conducted with high levels of accuracy. Some important conclusions are as follows:

- Mud rheology and cutting volume-fractions are the major sources of pressure drop in annulus. The increase in consistency coefficient in Herschel Bulkley model is the significant factor for increment of pressure gradient. The effect of high yield stress is not as significant, but showed sizeable pressure drop through annulus. Drill pipe rotation slightly reduces annular pressure drops. While inclination and eccentricity have minor effects on pressure drop, the results were contradictory between response surface types used. Therefore the effects of these two parameters cannot be safely deduced. The increase in flow rate significantly increases pressure drop. The introduction of cuttings have a profound effect on the pressure gradient. The effects of cuttings will be even larger if there is a cutting bed formation due to the reduced flow area.
- Kringing was consistently the best performing response surface model with Neural Network being a distant second. 2<sup>nd</sup> order Polynomials performed poorly for the analysis of drilling data.

## **5.2 Recommendation**

The project was achievable due to assistance from the Supervisor himself, Dr. Tamiru Lemma, in term of study material and introduction on ANSYS CFX software. Continued work on the HPHT effects on mud rheology will be needed in providing accurate analysis on the corresponding cutting transport regime.

- Further study is needed to reaffirm the effects of eccentricity and inclination.
- HPHT condition to be included for realistic prediction of the flow in the annulus. To do this, first we need developed empirical equation for viscosity and density as a function of temperature.
- Two-phase simulations with turbulence can be considered for the expansion of this study.

## REFERENCES

- [1] M. Duan, Miska, S., & Yu, M. , "Experimental Study and Modeling of Cuttings Transport Using Foam With Drillpipe Rotation," *SPE Drilling & Completion*, pp. 352-361., 2010.
- [2] M. A. Naamani, & Sharafi, M, "Drilling Optimization Benchmark Set for Deep HP/HT Wells in Oman," *E&P*, pp. 1-2, 2013.
- [3] P. H. I. Tomren, A.W.; Azar, J.j., "Experimental Study of Cutting Transport in Directional Wells," *SPE Drilling Engineering*, pp. 43-56, 1986.
- [4] H. Irfan. (2014, 10/2/2016). *History of Drilling Fluid*. Available: <http://www.enggpedia.com/chemical-engineering-encyclopedia/94-articles/1875-drilling-fluid-history>
- [5] T. R. Sifferman, "Hole Cleaning in Full-Scale Inclined Wellbores," *SPE Drilling Engineering*, pp. 115-120, 1992.
- [6] R. A. A. Sanchez, J.J, "The Effect of Drillpipe Rotation on Hole Cleaning During Directional Well Drilling," *SPE*, pp. 459-467, 1997.
- [7] P. E. Clark, "Drilling Mud Rheology and the API Recommended Measurements," *SPE*, pp. 933-940, 1995 1995.
- [8] R. Rooki, "Estimation of Pressure Loss of Herschel-Bulkley Drilling Fluids During Horizontal Annulus Using Artificial Neural Network," *Journal of Dispersion Science and Technology*, pp. 160-169, 2015.
- [9] M. E. H. A. A. Al-Majed, *Fundamentals of Sustainable Drilling Engineering* vol. 1: Wiley, 2015.
- [10] H. T. C. W. Pileh., "Yield-power law model more accurately predicts mud rheology," *The Oil and Gas Journal*, 1993.
- [11] K. K. M. Bourgoyne Jr., Martin E. Chenevert and F.S. Young Jr., *Applied Drilling Engineering* vol. 2. Texas: Richardson, 1991.
- [12] C. E. Brennen, *Fundamentals of Multiphase Flows* vol. 1. California: Cambridge University Press, 2005.
- [13] K. S. Ekambara, R. S., "Hydrodynamic Simulation of Horizontal Slurry Pipeline Flow Using ANSYS-CFX," *American Chemical Society*, pp. 8159-8171, 2009 2009.

- [14] E. G. S. H. Hashemabadi, "Numerical Study on Effects of Drilling Mud Rheological Properties in the Transport of Drilling Cuttings," *Journal of Energy Resources Technology*, vol. 138, January 2016 2016.
- [15] A. A. Pilehvari, "Generalized Hydraulic Calculation Method Using Rational Polynomial Model," *A Journal of Energy Resources Technology*, vol. 127, pp. 15-25, 2005.
- [16] J. M.-B. Hermosa, F., "Influence of Viscosity Modifier Nature and Concentration on the Viscous Flow Behavior of Oil-based Drilling Fluid at High Temperature," *Applied Clay Science*, pp. 14-21, 2014.
- [17] S. S. A. Okrajni, J.J., "The Effects of Mud Rheology on Annular Hole Cleaning in Directional Wells," *SPE Drilling Engineering*, pp. 297-308, 1986.
- [18] G. Thomas, "Transport Characteristics of Suspension: VII. A Note on the Viscosity of Newtonian Suspensions of Uniform Spherical Particles," *Journal of Colloid Science*, p. 1965, 267-277.
- [19] D. Babu, "Effect of P-p-T behavior of water muds on static pressures during deep well drilling," *Journal of Petroleum Science and Engineering*, pp. 341-355, 1993.
- [20] F. A. R. Pereira, Barrozo, M. A. S., and Ataide, C. H., "CFD Predictions of Drilling Fluid Velocity and Pressure Profiles in Laminar Helical Flow," *Journal of Chemical Engineering*, vol. 24, pp. 587-595, 2007.
- [21] G. Heng Yeoh, and Tu. J., *Computational Technique for Multiphase Flows*. New York: Elsevier, 2009.
- [22] E. Mitsoulis, "Annular Extrudate Swell of Pseudoplastic and Viscoplastic Fluids," *Non-Newtonian Fluid Mech.*, vol. 141, pp. 181-147, 2007.
- [23] M. E. Ozbayoglu, Saasen, A., Sorgun, M., and Svanes, K., "Critical Fluids Velocities for Removing Cuttings Bed Inside Horizontal and Deviated Wells," *Petroleum Science Technology*, vol. 28, pp. 594-602, 2010.
- [24] K. Founargiotakis, "Laminar, Transitional and Turbulent Flow of Herschel-Bulkley Fluids in Concentric Annulus," pp. 86-92, 2008.
- [25] H. T. Kummen, and Wold, A. A., "The effect of cuttings on annular pressure loss," Department of Petroleum Engineering and Applied Geophysics, Norwegian University of Science and Technology, 2015.

## APPENDIX-A

**Table-A1:** Rheological Models of Fluid

Model	Equations	Source
Newtonian	$\tau = \mu\dot{\gamma}$	Bourgoyne et al, 1991
Power law	$\tau = K\dot{\gamma}^n$	Bourgoyne et al, 1991
Bingham plastic	$\tau = \tau_y + \mu_p\dot{\gamma}$	Bourgoyne et al, 1991
Yeild Power Law (Herschel bulkley)	$\tau = \tau_y + K\dot{\gamma}^n$	Bourgoyne et al, 1991

**Figure-A1:** (a) FYP 1 Gantt Chart, (b) FYP 2 Gantt Chart, (c) Milestone

(a)

Activities	Weeks in FYP 1												
	1	2	3	4	5	6	7	8	9	10	11	12	13
1. Literature Review	█	█	█	█	█	█	█	█	█	█	█	█	█
Rheology			█	█	█								
Modelling					█	█	█	█	M1				
ROP Model							█	█	█				
HTHP Model										█	█	█	
2. Modelling and Simulation									█	█	█	█	█
Model Generation									█	█	█	█	M2
Meshing											█	█	
CFX Simulation, Validation												█	█
3. Parametrix Study													█
Effects of High Temperature													
Effects of High Pressure													



(b)

Activities	Weeks in FYP 2													
	1	2	3	4	5	6	7	8	9	10	11	12	13	14
1. Literature Review	■	■	■	■	■	■	■	■	■	■	■	■	■	■
Rheology														
Modelling														
ROP Model														
Pressure Gradient Predictions														
2. Modelling and Simulation	■	■	■	■	■	■	■	■	■	■				
Model Generation														
Meshing														
CFX Simulation, Validation														
3. Parametrix Study	■	■	■	■	■	■	■	■	■	■				
Influence of Mud Rheology	■	■	■	■	■									
Effect of Drilling Papameters				■	■	■	■	M3						
4. Documentation	■	■	■	■	■	■	■	■	■	■	■	■	M4	

(c)

No	Milestone	Date
M1	Benchmark model and fundamental equation selection	16/11/2015
M2	Modelling and simulation completion for the benchmark problem	9/12/2015
M3	Simulation and modeling of research problem	30/1/2016
M4	Further analysis of parametric study and final report completion	4/5/2016

**Figure A-2: Contour Plots of the validation test 1**

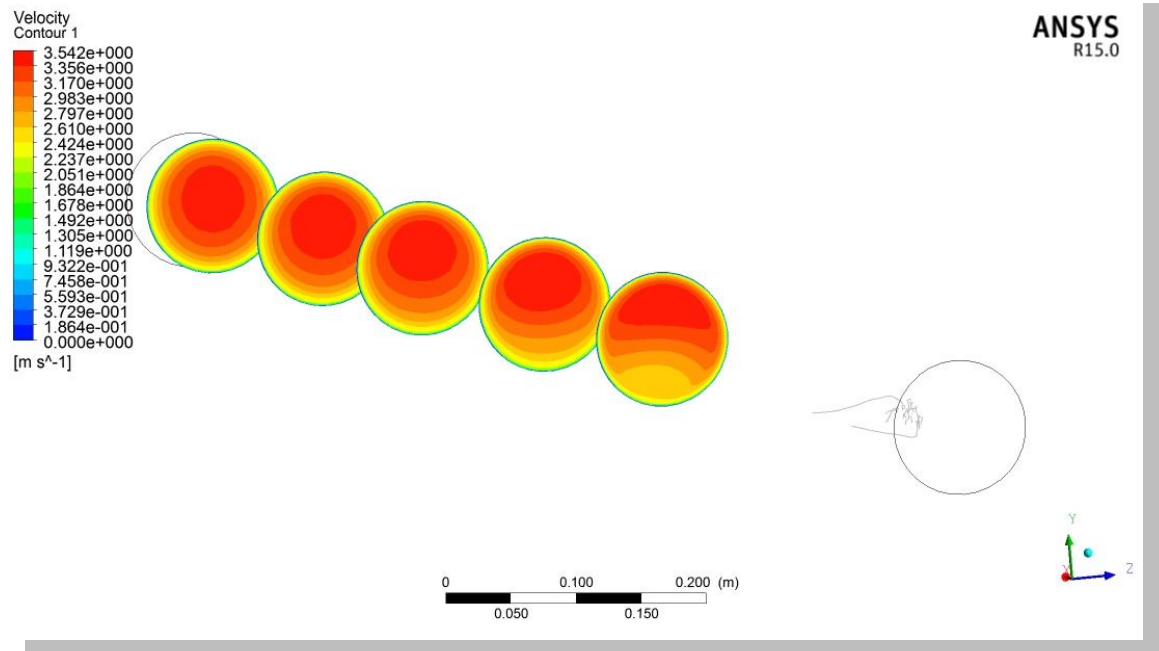


**Figure A-3: Point Cloud for Velocity – (a) without cutting, (b) with cutting**

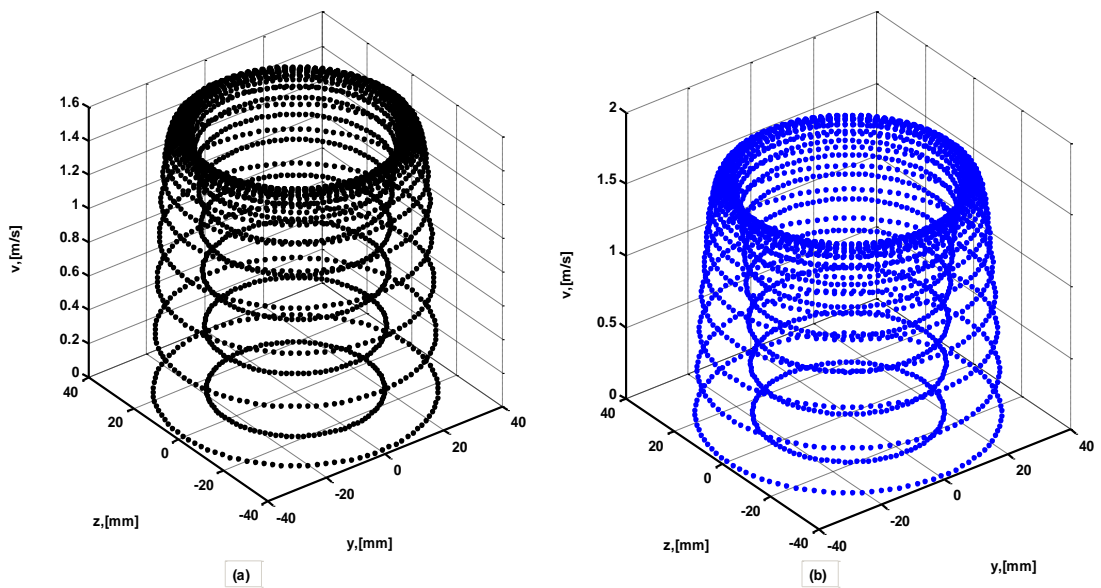


**Table-A2: Literature Review Summary**

Author	Objectives	Method/Results	Remark
GhasemiKafrudi (2016)	To study the hydrodynamics of mud-cuttings using the Mixture Model.	In-house code developed to calculate velocity and pressure fields. Mud velocity profile using Herschel-Bulkley model and solid phase volume fraction locally calculated with pressure drop though the annulus taken into account. Mud with high yield showed more pressure drop. Pressure drop increased by enhancing drillstring rotation. Maximum calculation error of 18% though friction factor calculation.	Only vertical annulus investigated. Eccentricity not considered. Mud velocity tested varied from 0.4 to 1.4 m/s. 12.25in hole simulated with 5in drillpipe
Duan (2007)	To investigate the effects of pipe rotation, foam quality and velocity, downhole pressure and temperature on cutting transport and pressure losses in horizontal well	Experiment parameters <ul style="list-style-type: none"> <li>- Backpressure 100-400 psi</li> <li>- Temp. 80 to 160 F</li> <li>- Rotary speed 0-120 RPM</li> <li>- Foam quality 60-90%</li> <li>- Foam Velocity 2-5 ft/sec</li> </ul> Pipe rotation significantly decrease cutting transport	First study of cutting transport using foam with pipe rotation. Includes pressure and temperature considerations.

		<p>concentration in horizontal annulus and reduces frictional pressure loss. Mechanistic model and associated computer simulator developed for practical and field application</p> <p>Model used to predict cutting concentration, bed height and pressure drop during horizontal foam drilling</p>	
Sorgun et al (2015)	To predict pressure loss of Newtonian and Non-newtonian fluids with CFD and Support Vector Regression (SVR)	<p>SVR and CFD results compared to data from literature. Comparisons show CFD better for Newtonian fluids (3.48% vs 19.5%). SVR could predict frictional pressure loss with AAPE less than 5.09% for Newtonian and 5.98% for non-Newtonian fluids. Rotary pipe has no effect on frictional pressure loss of Newtonian fluids for concentric annulus. Increased pipe rotation causes less frictional pressure drop for non-Newtonian fluids.</p>	<p>SVR good for both Newtonian and non-Newtonian fluids. SVR not effected by outlier points as much as regular regression equation.</p>
Rooki (2005)	To predict pressure loss of	Average relative error was less than 5% with	

	Herschel-Bulkley Drilling fluid in concentric and eccentric annulus using Artificial Neural Network (ANN) method	correlation coefficient (R) of 0.999 for predicting pressure loss. Experimental data from literature review used to train ANN to predict pressure loss. Model performance determined by AAPE.	
Pilehvari et al (2005)	To produce hydraulics model using a generalized hydraulics calculation technique	Uses rheological model called Rational Polynomial Model. Model capable of accurately representing rheogram of virtually any time-independent fluid. Prediction of models compared to published experimental data. Cases include laminar and turbulent flow for varying drilling fluid in concentric fluid.	Capable of predicting pipe and annular flow pressure drop in laminar and turbulent region. Model suited for correlating equation in general computer program for hydraulic calculation
Ekembara et al (2009)	To investigate the effect of in situ solid volume core, particle size, mixture velocity, and pipe diameter on solid concentric	ANSYS-CFX used for simulation. Behavior of slurry pipeline flow predicted using transient 3D hydrodynamics model based in kinetic theory of granular flow. Experimental and simulated results show	CFD model doesn't need experimental data to tune. Considered better than correlation-based

	<p>profiles, particles, liquid velocity profiles and frictional pressure loss.</p>	<p>particles asymmetrically distributed in rational plane. Degree of asymmetry increases with increase in particle size. Once particle size large enough, concentration profiles dependent only on in situ solid volume fraction</p>	<p>empirical models.</p>
--	--	--	--------------------------